USING A TRACER TEST TO ASSESS THE TRANSPORT AND FATE OF NITRATE IN A SATURATED BUFFER ZONE

ALHASSAN SAHAD

51 Pages

The Upper Mississippi Basin (UMB), which includes Illinois, has highly fertile soils and therefore, experiences intensive agricultural practices. While fertile, the soils do not drain well, resulting in the installation of tile-drainage systems. Agricultural practices within the UMB involves the application of nitrogen (N)-rich fertilizers. The tile systems coupled with the application of N fertilizers have led to the excessive export of nitrates as nitrogen (NO_3-N) from the agricultural fields into surface and subsurface waters through subsurface tile drainage systems. Excess NO_3-N contributes to eutrophication and to development of hypoxic zones in aquatic environments. One method that has exhibited success in lowering NO_3-N concentration is the diversion of tile drained waters from the agricultural fields into a saturated buffer zone (SBZ) before the water enters a stream. A SBZ is an area of perennial vegetation between agricultural fields and water ways where a tile-outlets drain. The SBZ serves as a sink where NO_3-N is lost through natural processes such as plant uptake, denitrification, and dilution with groundwater. Previous works have shown a decrease in the NO_3-N content in the SBZ, but the extent to which this removal occurs cannot be quantified without knowing the travel time of the water through the SBZ. Our goals were to use sodium bromide (Nar) and sodium chloride (NaCl) as tracers to determine the travel time of the tile waters in a SBZ at the T3 site in Hudson, Illinois and to quantify the amount of loss or dilution of the NO_3-N in the SBZ using a mixing model.

The travel times of NO_3-N from diversion tiles to wells ranged from 7 days to 17 days. Results from the tracer test show an average groundwater velocity of 0.36 m/day with a standard deviation of 0.18 m/day, using the arrival time of the chloride tracer. The travel time from the SBZ to the stream is 27 days which corresponds to 43% NO_3-N removal from the mixing model. This research further reinforces the effectiveness of using SBZ as NO_3-N reduction strategy.

KEYWORDS: Nitrate, Saturated Buffer Zone, Travel Time, Plant Uptake, Mixing Model

USING A TRACER TEST TO ASSESS THE TRANSPORT AND FATE OF NITRATE IN A SATURATED BUFFER ZONE

ALHASSAN SAHAD

A Thesis Submitted in Partial
Fulfillment of the Requirements
for the Degree of

MASTER OF SCIENCE

Department of Geography, Geology, and the Environment

ILLINOIS STATE UNIVERSITY

2022

USING A TRACER TEST TO ASSESS THE TRANSPORT AND FATE OF NITRATE IN A SATURATED BUFFER ZONE

ALHASSAN SAHAD

COMMITTEE MEMBERS:

Eric W. Peterson, Chair

Wondy Seyoum

Catherine O'Reilly

ACKNOWLEDGMENTS

I would like to express my profound gratitude to my supervisor Dr. Eric Peterson for his support and encouragement in this project. One of the best things I learned from Eric is how down-to-earth he is and how is willing to explain basic concepts to students without letting the students feel dump. He helped me a lot in understanding the theoretical and the experimental set up of this research and hydrogeology in general.

I want to thank my committee members Dr. Wondy Seyoum and Dr. Catherine O'Reilly for their advice and guidance throughout this research. I want to thank Dr. Catherine O'Reilly for training me in the use of IC and analysis of samples.

I would like to thank the city of Bloomington for access and logistics support. I would also like to thank Illinois State University Department of Geography, Geology, and the Environment for their support.

Finally, I would like to thank many of the graduate students and the 2021 GEO 456 students who helped in conducting slug tests on the site during the summer. Special thanks to Eli Schukow and Joe Hoberg for their help during the test and sample collection.

A.S.

CONTENTS

TABLES

FIGURES

CHAPTER I: INTRODUCTION

Nitrate in the Environment

Agriculture is known to be one of the leading causes of surface water pollution (Anderson et al., 2014), serving as the principal source of various types of nutrients such as nitrogen (N), primarily nitrate as nitrogen (NO_3^--N), and phosphorus(P) to aquatic environments. N is among the primary nutrients required for the growth and development of plants but is also a major groundwater and surface water pollutant that has become an environmental problem of widespread concern (Castaldelli et al., 2019; Xin et al., 2019; Zhang et al., 2018). As farmers seek to meet the global food demand, the amount of available N in the terrestrial cycle has doubled with agriculture being the most contributing factor (Anderson et al., 2014; David et al., 2010; Galloway et al., 2003). N fertilizers and organic nitrogen in manure are major sources of nitrogen pollution, as crops do not assimilate all of the applied N (Lutz et al., 2020).

The Midwest of the United States has experienced a dramatic rise in fertilizer and pesticide use since the mid-20th century. The Mississippi River Basin in the Midwest contains some of the highest concentrations of nonpoint source NO_3^--N in the United States. Accumulation of NO_3^--N in aquatic environments has negative effects, which include development of algal blooms, creation of hypoxic zones, and degrading drinking water quality (USA Environmental Protection Agency,2018). The hypoxic zones and algal blooms in the Gulf of Mexico and Lake Erie are clear manifestation of the negative impact of NO_3^--N export into water bodies. Additionally, excessive accumulation of NO_3^--N can cause health effects in freshwater systems, including biodiversity changes and the death to some aquatic organisms (David and Gentry, 2000). According to (Keeney and Hatfield,2010), the Illinois River contributes from 15% to 20% of the total nitrogen that goes into the Gulf of Mexico from the Mississippi River.

The upper Mississippi River basin, which includes Illinois, has some of the most fertile soils, and hence, agricultural practices are very prevalent in this area. Illinois farmland covers 27 million acres, which is approximately 75 percent of the state's total land area (Illinois Department of Agriculture 2020). Grain crop yield is enhanced through the addition of nitrogen from sources such as manure and fertilizer (Fernandez et al. 2009, Quyang et al. 2018). Approximately 7.7 billion kilograms of N-fertilizer are applied to Illinois corn fields annually (United States Department of Agriculture 2018). The NO_3^-N from N from these fertilizers ultimately finds themselves into the streams and other water bodies both within and out of Illinois.

The processes by which nitrate is introduced into the soil and its movement as well the pathways that it takes within the soil are best explained using the nitrogen cycle as shown in fig. (1).

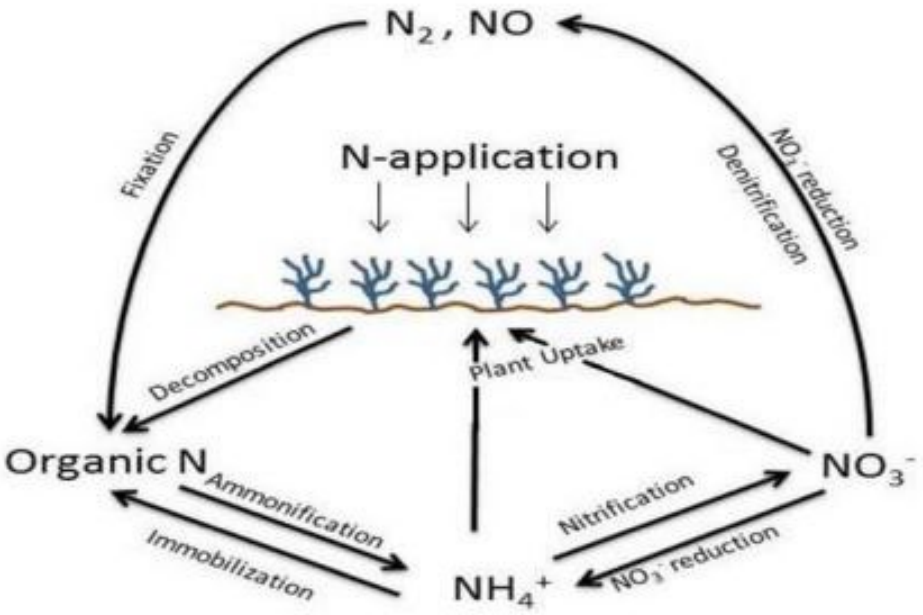

Figure 1: The Nitrogen Cycle

Within the soils of the Midwest, specifically Illinois, there is generally high-water table, and this does not support the growth of most crops. Excessive soil moisture stunts plant growth due to an oxygen deficiency in the root zone and a reduction in nitrogen uptake resulting from denitrification and leaching (Kaur et al., 2017). To improve soil drainage and maximize crop yield, extensive channelization, and installation of subsurface draining systems (tiles) have been initiated across most farmlands in the Midwest (Fausey et al.1995). The tiles drain the soil water above it directly into streams or ditches giving little opportunity for denitrification, plant uptake, and microbial immobilization to take place to naturally remove the excessive NO_3-N from the tile waters. Within the soil, processes such as ammonification, immobilization, nitrification, and denitrification can transform nitrogen into different and often harmless forms (Sylvia et. al, 1998). Tiles short-circuit the roles of the soils in the nitrogen cycle and contribute to pollutants in surface streams, and with that the potential for the removal of nitrate is lost in the soil. While the installation of tile drains has been highly successful by opening additional lands for agricultural developments and increasing crop yield, the short-circuiting process directly contributes 52% of NO3-N entering the Gulf of Mexico (David and Gentry, 2000). It will be impractical to remove the tile drains to protect water bodies from pollution because of their immense contribution to crop yield. So, a compromise must be made to lessen the effect of tile drains and work around them

To reduce, mitigate, and control hypoxia in the Northern Gulf of Mexico and to improve water quality in the Mississippi River Basin, a national strategy action plan was introduced in 2008 (United States Environmental Protection Agency, 2007). The state of Illinois developed their own plan known as Illinois Nutrient Loss Reduction Strategy (NLRS) released in 2015 to improve water quality, not only in Illinois, but downstream, to reduce hypoxic zone in the Gulf

of Mexico (Illinois NLRS Biennial Report, 2019). The strategy sets long-term goal of reducing loads from Illinois for total nitrogen and total phosphorus by 45% with interim reduction goals of 15% of NO_3^-N and 25 % total phosphorus by 2025 (Illinois NLRS Biennial Report, 2019). There are five main best management practices that have been proposed to reduce the export of nitrate. These practices are free water surface constructed wetlands, denitrifying bioreactors, controlled drainage, saturated buffer zones, and integrated buffer zones(Carstensen et al., 2020)

Saturated Buffer Zone

One practice of the NLRS, which has shown a great promise in reducing the NO3-N export, is the diversion of tile drained water into a riparian buffer zone, creating a Saturated Buffer Zone (SBZ). A buffer zone is a land that is situated between an adjacent stream and an upland ecosystem(Gregory et al., 1991). In a SBZ, drainage water and riparian soil are reconnected by a buried , lateral perforated distribution pipes (diversion tiles) running parallel to the stream, which redirect the tile-drainage water into the riparian zone (Carstensen et al., 2020). The infiltrating water saturates the riparian soil creating anoxic conditions (Carstensen et al., 2020).The lowering of the NO3-N concentrations in the SBZ has been associated with denitrification, assimilation, and dilution (Jaynes and Isenhart 2014). Denitrification, the process where NO3-N is converted into dinitrogen (N_2) through microbial metabolism results in permanent loss of N as N_2 to the atmosphere (Zumft 1997), while assimilation, the process by which NO3-N is taken up by plants through their roots, serves as a short-term sink (Bosompemaa et al., 2019). Dilution occurs as the result of the reintroduction of high concentration tile water into the low concentration groundwater system.

Several studies have been conducted to assess the effectiveness of SBZ as a NO_3 reduction strategy. In the Midwest, widely implementing SBZs could result in a 5 to 10% reduction of the estimated N load from tile-drained from tile-drained land (Chandrasoma et al., 2019). Jaynes and Isenhart (2018) monitored nearly 20 SBZs in Iowa finding an average of approximately 50% of the annual drainage volume was treated within the buffers and nearly an average of 83% of the nitrate within that water was removed. Additionally, Groh et al. (2018) carried out a study in the Midwest on two SBZ and indicated about 96% of the total diverted nitrate rich waters from the tile drainage was removed. Furthermore, 15 SBZs across the Midwest were monitored by Brooks and Jaynes (2017) from September 2016 to February 2017, and they observed 61% loss of nitrate loading. Also, In the first study of the practice of SBZs, Jaynes and Isenhart (2014) installed a SBZ on an outlet draining 10.1 ha of a row-cropped field in Iowa. Over 2 years, they measured that 55% of the total flow from the outlet was redirected into the buffer as shallow groundwater. Contained within the water was 228 kg N as NO_3. Given the reductions in NO3 concentrations in the shallow groundwater as it seeped toward the adjacent stream, they concluded that all 228 kg N of NO3 that entered the buffer was removed and that no measurable NO3 reached the stream Even though the SBZ method of nitrate reduction have been studied extensively, there is still a problem of lack of knowledge on the travel time of the water within the SBZ. Knowing the travel time will help better understand and quantify the importance of SBZ in NO3-N removal. For example, longer travel time implies that the redirected tile water gets enough time in the SBZ to undergo the natural processes needed for NO3-N removal.

Research Questions and Hypothesis

The goal of this study is to answer the following research questions:

1. What is the travel time of tile waters within the SBZ?

2. To what degree is NO_3-N removed from the SBZ?

To the understand the research questions, two hypotheses were addressed:

1. The travel time of tile water from diversion tiles farther away from wells will be longer than those from diversion tiles closer to wells.
2. The amount of reduction of NO_3-N will increase as one moves away from a diversion tile.

CHAPTER II: METHODS

Study Site Description

Site T3 is herbaceous saturated buffer located 3 km north-west of Hudson, Illinois (40.614382˚N, 89.023542˚W) that receives agricultural runoff from a farm located approximately 120 m to the east (fig.2). There is a third order stream (T3 stream) that lies at the far west of the study site. The stream drains into Evergreen Lake, northwest of Hudson, Illinois, which serves as a source of drinking water as well as a recreational area to the City of Bloomington. Growth of terrestrial plants begin in early to mid-spring, flowering occurs from mid-spring to early summer, and seed maturity is reached by mid to late fall (Ogle et al., 2002). The study site has been outfitted with an agricultural treatment system that directs a portion of tile water (agricultural runoff) into the subsurface within the saturated buffer area. The agricultural runoff is directed into 3 perforated diversion tiles 1 m below the surface by a diversion system, while the remaining volume is discharged directly into the stream (Tributary 3 or T3) when there is an excess run off. The diversion box consisted of three chambers separated by a set of stoplogs. The stoplogs were used to control the elevation of the water flowing from the upstream chamber into the middle chamber and from the middle chamber into the downstream chamber and stream Within the study site, there are thirty-five observation wells are installed; each well has a 0.75 m screen. One set, which is parallel to the groundwater flow, consists of 6 sets of nested wells namely 2,4,6,8,10 and 12 with four wells(A-D) at each nested station. The C and D have depth of 2.3 and 1.5 m respectively and are for collecting shallow (from 0-2m depth) groundwater samples. The A and B wells are installed to a depth of 3.8 m and 3.0 respectively and are for collecting deep (depth below 2m) groundwater samples. The other sets of wells are composed of eleven individual wells screened at 2.3 m each

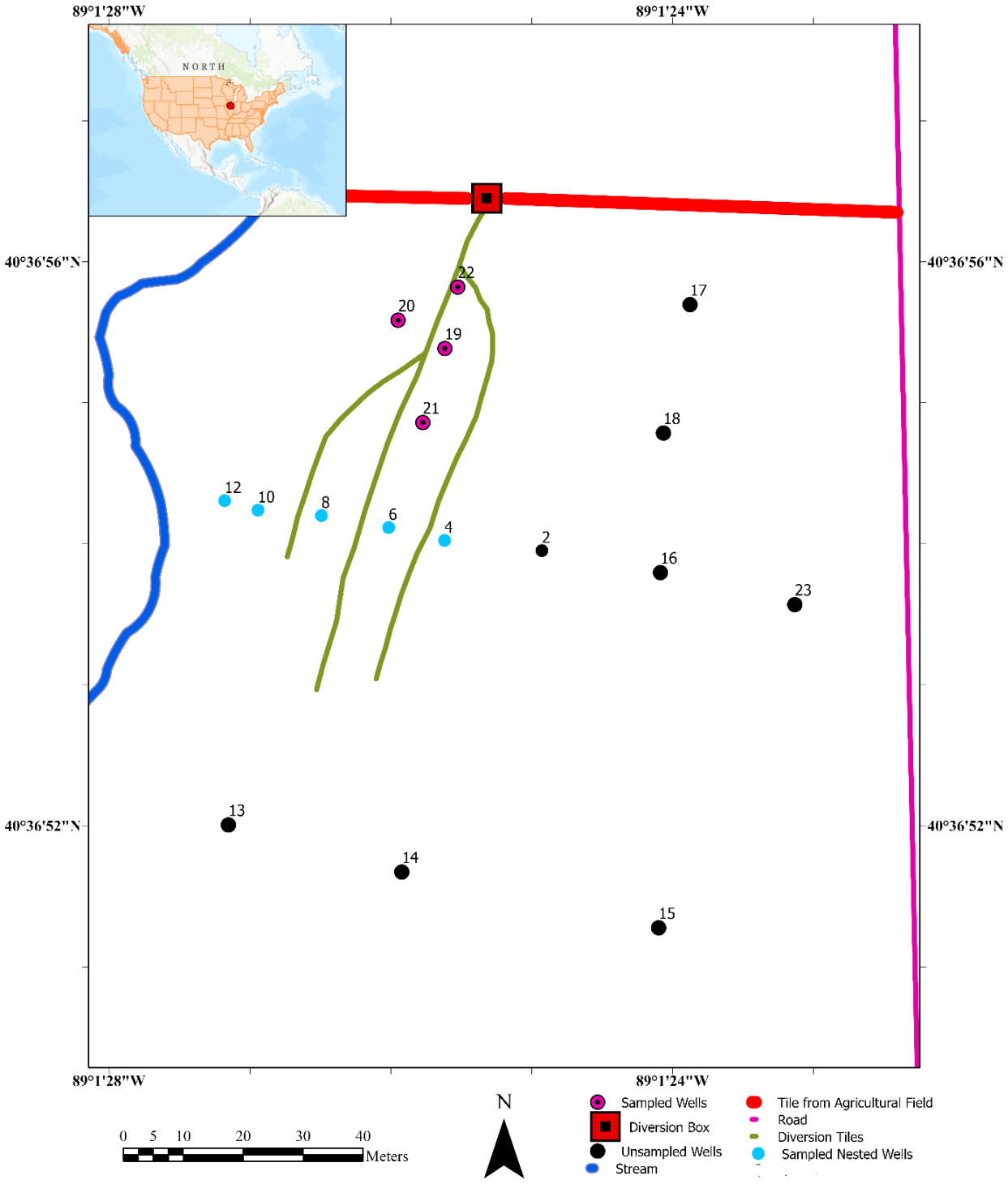

Figure 2: Study Site Showing monitoring wells, diversion tiles and stream(T3). The sampled wells are 4C,6,8,10,12,19,20,21 and 22.4C was used as the background well

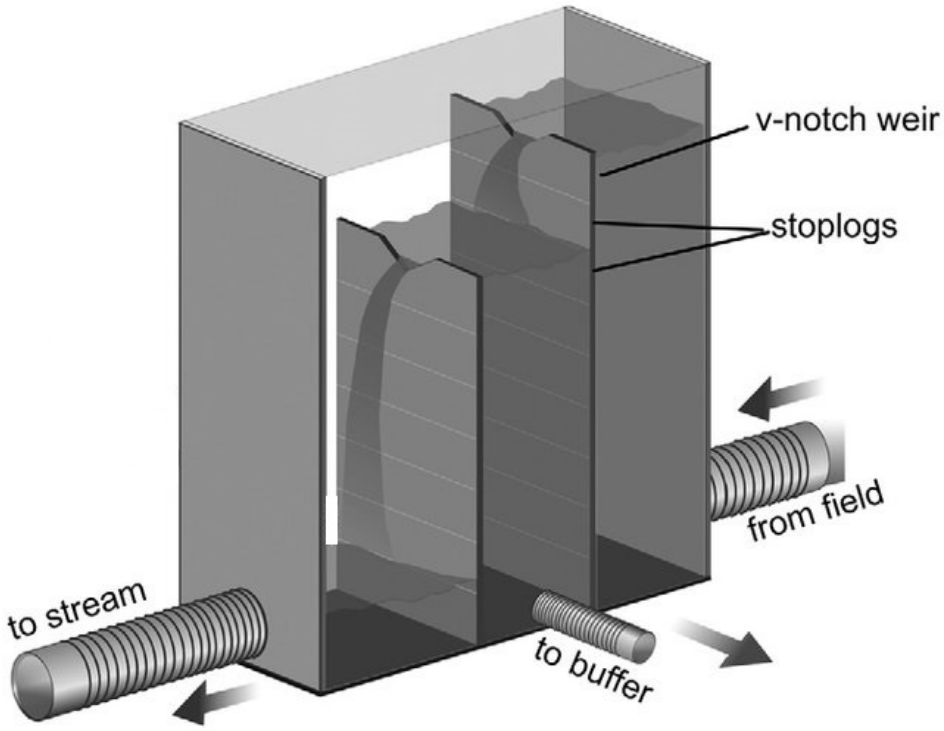

Figure 3: : Schematic of the diversion box showing how tile water is diverted into the SBZ (modified from Jaynes et. al, 2011)

Geology

Throughout the site, the surface (0-0.63 m) is dark organic-rich topsoil, which is underlain (0.66-1.5 m) by a firm clay loam composed of silty clay, clay, and sandy clay. The clay loam is graded with an increasing sand gravel percentage with depth which into transitions to a coarse-grained material composed of a gravely silt with sand, sandy silt, and clayey sand from 1.5 m to 2 m. The thickness of this coarse-grained zone varies spatially. The coarse-grained material is underlain by blue-grey, dense diamicton belonging to the Tiskilwa Till member of the Wedron Formation deposited during the Wisconsinan glaciation (Weedman et al., 2014). The thickness of the diamicton is 30-45 m terminating at Silurian dolomite bedrock (Wickham, et al., 1988). A

simplified cross section through the various geological units running parallel to the groundwater flow of the study site is shown below.

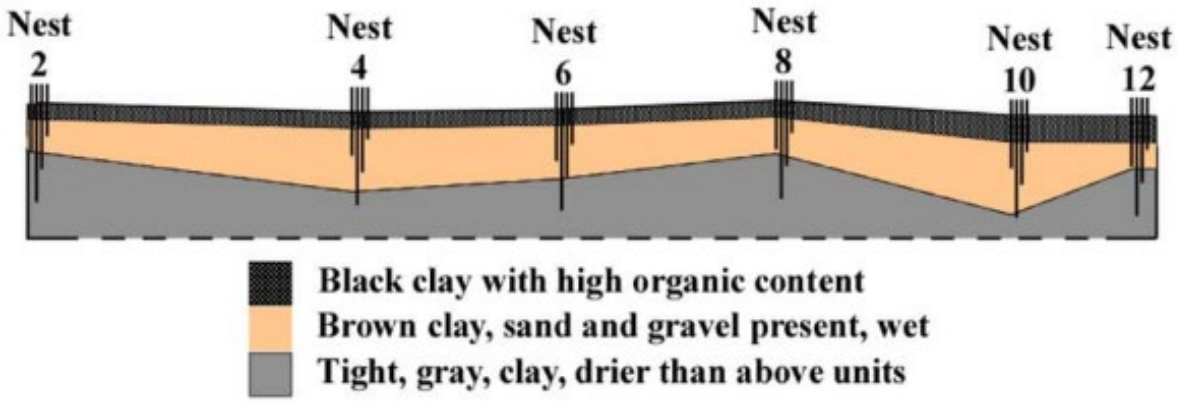

Figure 4: Cross section of the soil profile at the study site. included with the nested wells, (modified by Peterson et. al, 2015)

Hydrological Setting

Groundwater flow is from east to west, with flow towards the stream T3(fig5). The average monthly precipitation for the last 40 years was highest in spring and lowest in winter with a yearly average of 950 ± 100 mm (Bastola, 2011; Changnon et al., 2004). The tiles start running from late winter (March) to late spring (end of May – early June) and again in fall. The average hydraulic conductivity (K) obtained from slug test is 2.2×10^{-5} m/s. At a depth of 1 m, the average porosity is 0.32 (Sanks et al. 2015). Surface water infiltrates to the sand and gravel zone where it then flows horizontally. Waters in the sand and gravel zone are a bicarbonate rich water as compared to waters derived from the till, which are sulfate rich (Akara et al., 2015). The sand and gravel waters represent the shallow waters, while the waters obtained from the till are deep waters. Through the study area the shallow and deep aquifers do not mix, except for areas around

wells 10, 12, and 20, where upwelling of the till derived waters has been documented (Akara et al. 2015). The regional groundwater gradient is from SE to NW towards the Mackinaw River. The depth to groundwater is approximately 2m during the dry season and less than 0.5 m during the rainy seasons.

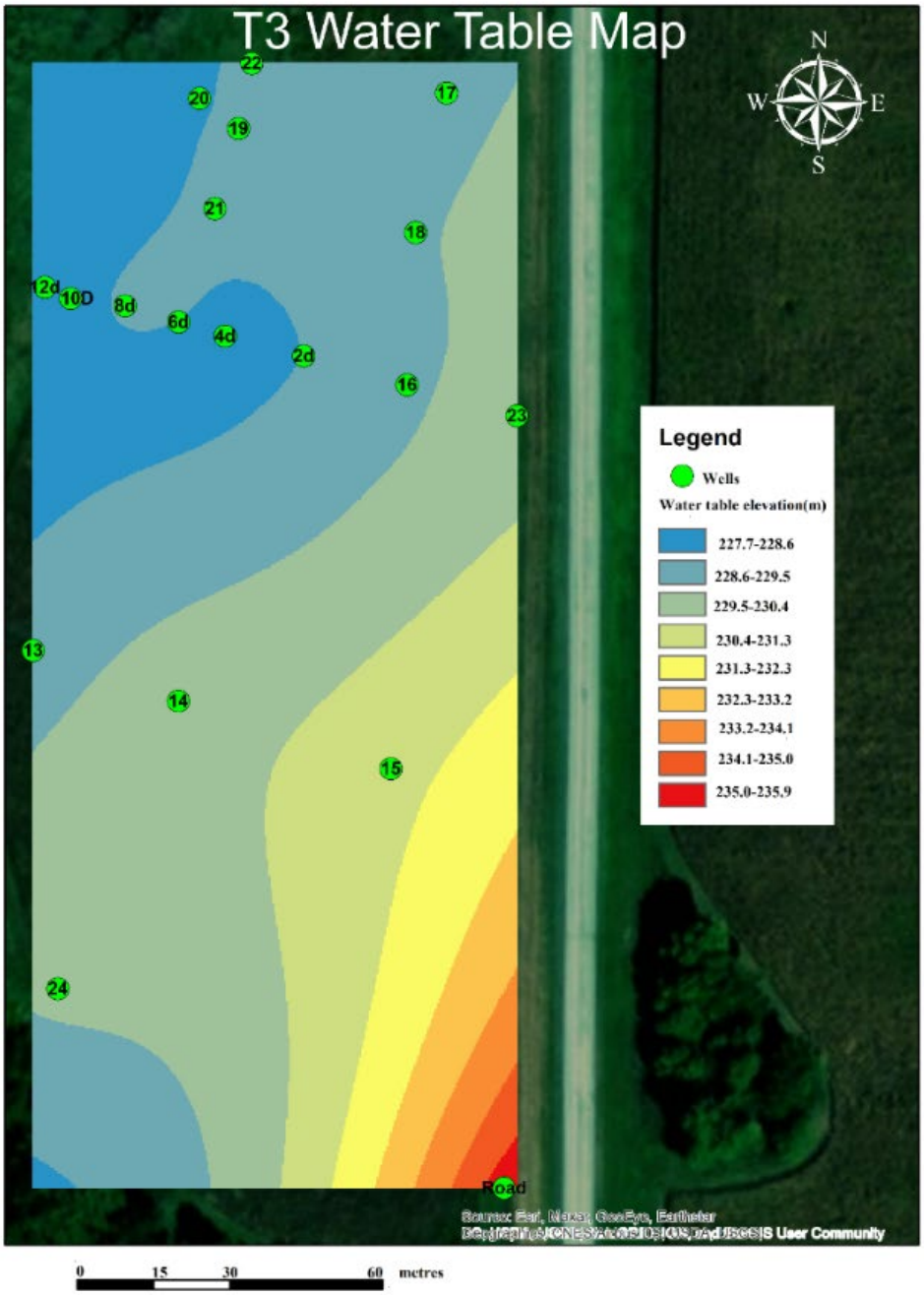

Figure 5: Water Table Elevation at T3, May 2021, groundwater moves from southeast to northwest

Tracer Test

Groundwater samples were taken from the wells within the SBZ as well as the diversion box prior to the start of the tracer test to ascertain the background concentration of the major anions (Cl^-, Br-, SO_4^{2-} and NO_3-N) Water quality parameters such as the pH, conductance, specific conductance, and dissolved oxygen were also recorded. These parameters gave a general geochemical behavior of the groundwater. The static water levels were recorded at each sampling event to determine the groundwater flow directions.

A tracer test was conducted within the SBZ in the spring of 2021. The tracer test started on the 13th of March 2021 after there was an appreciable amount of water flowing through the tile. Sodium chloride (NaCl) and sodium bromide (NaBr) were used as tracers for the tracer test. NaCl and NaBr were chosen because the background concentration of Br lower in the study area and because of the conservative nature of the tracers. A hydrogeological tracer test interpretation software known as TRAC (citation) was used to calculate the appropriate masses that will cause an appreciable change in concentration of the system. Six (6) Kg of NaCl and 4 Kg of NaBr were thoroughly mixed with water separately until both were completely dissolved. The solution of the tracers was injected into the upper compartment of the diversion box to allow for additional mixing of the tracers before the solution moves into the middle compartment where it is directed into the SBZ through a diversion tile.

Pre- and Post-Tracer Test Sampling

Groundwater samples were taken from the wells within the SBZ as well as the diversion box prior to the start of the tracer test to ascertain the background concentration of the major anions (Cl^-, Br-, SO_4^{2-} and NO_3-N) Water quality parameters such as the pH, conductance, specific

conductance, and dissolved oxygen were also recorded. These parameters gave a general geochemical behavior of the groundwater. The static water levels were recorded at each sampling event to determine the groundwater flow directions. involved the measurement of the water quality parameters using a YSI probe. These water quality parameters are pH, electrical conductance, specific conductance, and percent dissolved oxygen. The static water level was measured using a water level indicator. Prior to sample collection, the wells were purged using a bailer to ensure aquifer water rather than stagnant well water was collected. About 3 liters of water were purged from each well, and the wells can refill to an appreciable level before the sample is taken. A 60 ml sample was taken from each well. The samples taken from each well were filtered through one (1) µm pore space fiber membrane filter to remove large particles before the analysis by the ion chromatograph (IC) was done. Samples were analyzed for major anions: fluoride, chloride, bromide, nitrate as nitrogen, phosphate, and sulfate, using an IC. Prior to the testing, the samples were frozen if there were not tested on the same day they were collected from the site. Quality assurance (QA) and quality control (QC) were maintained during the analysis by running continuing calibration verification (CCV), blanks and duplicates and the making the analytical error was less than 3%.

Groundwater sampling started three (3) days after the initiation of the tracer test. Initially, the planned sampling frequency was one week; however, following the second sampling (Day 10 after injection), the sampling frequency was increased to three times a week. The frequency of the sampling was increased when the concentration of the $Cl^-$and Br^- started increasing and detected minor changes in concentration.

Each sampling event followed the same protocol as with the pre-test sampling. Samples were taken from wells 4C, 4D, 6C, 6D, 8C, 8D, 10C, 10D, 12C, 12D, 19, 20, 21, and 22 during the 25-day duration of the study. Wells located upstream of the diversion tiles were not affected by the tracer and therefore was not sampled. Wells 4C and 4D were sampled even though they were not affected because that was needed to be the groundwater end member the mixing.

Determination of Travel time

The movement of the chloride was used as a proxy for the nitrate, and therefore, the travel time of the NO_3-N. To determine the travel time of the NO_3-N within the SBZ, breakthrough curve analysis was used. Travel time in this sense is the amount of time NO_3-N takes to travel from a diversion tile to a well or the stream. Travel times from diversion wells to stream will be calculated using breakthrough curve analysis and quantified using the curve generated from the change in concentrations of the tracer ions as they enter the wells from the diversion box (break through curves). The concentration of the tracer ions in the well is expected to shoot up once the tracer ions get to well and the travel times will be calculated from the breakthrough curve as the time where the maximum concentration of the tracer was achieved.

Using the hypothetical graph shown below (fig 4), the mean velocity ($\bar{v}$) of flow of the tile water from a diversion tile to a well (fig 3) was calculated as:

$\bar{v}$= (distance from tile to well)/(T_p) eq. 1

where T_p is the time to peak of the breakthrough curve. The hydraulic conductivity (K) was determined from Darcy's Law:

$K=(\bar{v}*n)/(i)$ eq. 2

Where n is the effective porosity of the aquifer, taken as 3.2% (Sanks et al., 2015), and *i* is the hydraulic gradient. The hydraulic gradient was calculated from as the difference between two

selected groundwater head values to the actual distance between them on the ground and it was assumed to be constant, during the tracer test, the *i* was 0.002 m/m. The hydraulic conductivity calculated form Darcy's Law was then compared to slug test derived K values to ascertain the accuracy of the results obtained from the tracer test.

The Darcy's velocity gives the mean velocity of flow of the Cl from of the tile water to the closest well. The travel time of the tile water from a diversion tile to the stream is then calculated.

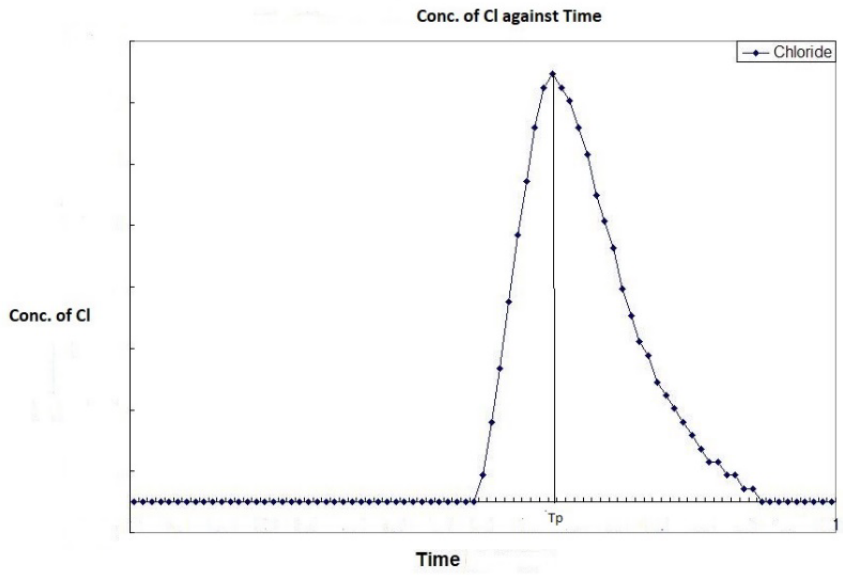

Figure 6: Breakthrough curve of a typical Chloride Tracer Test, Tp is the peak time-the time the chloride tracer arrives in the well

The distances from the wells to the closest tiles of influence was determined using the path that followed the steepest gradient. The hydraulic gradient was determined using the slope of the water level elevation. The point measurements of the hydraulic head were done using the inverse distance weighting method. The slope function in ESRI ArcGIS was used to determine the slope of the head of water.

Mixing Model

A two-component mixing model was used to assess whether the concentration of NO_3-N has been diluted, whether there has been a loss or gain of mass, or whether there has been an addition of NO_3-N into the system. The end members are the water from the groundwater system, waters from the upgradient well 4C, and water from the diversion box. The mixing model was developed using chloride as a conservative tracer; the proportion of the groundwater mixing with the tile in the SBZ was determined using the method proposed by Triska et. al (1989). The quantity of water at an observation well (Q_w) will theoretically comprised of two sources: water from the tile (Q_t) and water from the groundwater system (Q_g).

$Q_w = Q_t + Q_g$----------(3)

Employing conservation of mass equations to calculate the proportion of tile water mixing with the well water ($\frac{Qt}{Qw}$)

$Q_w Cl_w = Q_t Cl_t + Q_g Cl_g$----------(4)

$$\frac{Qt}{Qw} = \frac{Clw - Clg}{Clt - Clg}$$ ----------(5)

Where Clw is the concentration of Cl^- in the well water. Clg is the concentration of Cl^- in groundwater and Cl_t is the concentration of Cl^- in the tile water. Water from well 4C was used as the groundwater end member because it was unaffected by the tile water from the diversion box. Assuming a conservative nature for NO_3-N and substituting the concentration of NO_3-N for Cl^- in the well water, groundwater and tile water, and rearranging eq. (3) to solve for NO_3-N N in each well:

$$NO3\text{-}N = \left[\frac{Qt}{Qw} \times (NO3t - NO3g)\right] + NO3g$$ ----------eq. (6)

The concentrations calculated with eq (6) represent the theoretical NO_3-N concentration assuming dilution is the only. Deviations in NO_3-N concentrations indicate either a removal (modeled – measured resulting in a positive number) or addition (modeled – measured resulting in a negative value) of NO_3-N along the travel path. The amount of reduction (or addition) of NO_3-N can then calculated using

$$\frac{\mathrm{NO3{-}N\ (modeled){-}NO3{-}N\ (measured)}}{\mathrm{(NO3{-}N\ (modeled))}} \times 100 \text{----------eq. (7)}$$

The mixing model treats NO_3-N as a conservative solute, and eq. (6) provides the predicted NO3-N concentration assuming the only controlling process is dilution. However, NO_3-N is not conservative and can be added and removed from the system via nitrification or denitrification or plant uptake, respectively. Thus, difference between the NO3-N concentrations generated by eq. (4) and the measured NO3-N concentrations quantify the loss or gain of NO3-N from the water as it travels from the diversion to the observed wells. If the measured NO3-N concentration is greater than the modelled concentration from eq. (3), then it implies there is addition of NO3-N However, if the measured concentration is less than the modelled concentration, it implies nitrate removal, which could be due to denitrification or plant uptake and when the measured concentration and the modelled concentration are the same, it implies there is dilution from groundwater.

CHAPTER III: RESULTS

General Tracer Data

The tracer test started on the 13th of March 2021. The first sampling post injection occurred 3 days later 16th March. While both Cl^- and Br^- data were collected from the well water. only the Cl data were used because Br^- concentrations were below detection limit (BDL), and the concentration of the Cl was observed above the background concentration to be useful in the tracer test analysis. The addition of 4 Kg of Na Br was unable to raise the concentration of Br above the background. A rainfall event occurred on the 25th day following the initiation of the test. This storm altered the breakthrough curves of Cl, generating a second peak of Cl in the wells days after the precipitation event. As a results of the rain event, the mixing model was only employed to day 26.

Dissolved oxygen Data

The dissolved oxygen (DO) in the wells was measured during each day of the sampling during the tracer test with a YSI probe. Results from the DO were used to assess the anoxic conditions of the ground water and hence the possibility of denitrification occurring or not. Generally, the DO ranges from 0.75 mg/l to 10.30 mg/l with an average of 4.33 mg/l. The table below gives a general overview of the DO (mg/l) data collected during the test.

Table 1: Dissolved Oxygen Concentration in mg/l

Well	min	Mean	max	Standard Deviation
4C	1.04	2.03	3.39	0.70
4D	0.75	1.51	2.22	0.43
6C	1.11	4.75	7.22	1.63
6D	1.21	2.90	7.86	1.76
8C	1.35	4.79	6.21	1.35
8D	1.76	4.93	7.56	1.54
10D	2.11	6.60	8.37	1.93
12C	1.17	4.49	5.69	1.28
19	3.14	0.45	9.46	2.16
20	0.88	7.06	10.30	2.29
21	0.98	5.30	3.14	0.65
22	2.67	2.00	9.12	1.85

Chloride Data

The concentration of the Cl- used in the test started from the background concentration and then increased gradually till it got to a peak and then back to the background concentrations. This is what is expected from any given tracer test; however, the effect of precipitation can change this general expectation from the tracer test.

The concentrations of the Cl^- in the groundwater, as measured from the wells downstream of the diversion tile, ranged from as low as 2.02 mg/l to a maximum of 15.3 mg/l. The concentration of the Cl^- generally started from the background concentration and increased as the mass of the

tracer approached the wells. Table 1 shows the descriptive statistics of the concentration of Cl^- in the wells sampled during the tracer test.

Table 2: Descriptive Statistics of the concentration of chloride measurement mg/l

Well	Min	average	Max	standard deviation
4C	3.13	4.08	6.29	0.79
4D	2.57	3.40	8.93	1.76
6C	2.14	3.13	6.45	1.11
6D	2.02	2.78	6.19	1.11
8C	2.66	4.95	11.02	2.48
8D	2.86	4.61	9.63	2.15
10C	4.63	6.93	10.25	1.80
10D	4.35	10.12	14.59	2.35
12C	5.97	10.00	15.33	2.35
12D	6.87	10.39	15.21	2.04
19	5.00	6.85	12.51	2.55
20	8.72	10.89	13.54	1.38
21	6.80	9.31	12.63	1.40
22	4.94	6.32	11.73	2.05

As a result of the storms on the on 26th day after the tracer injection, breakthrough curves for the waters at the sampled wells displayed multiple peaks. The arrival times were taken from the first peak, which also exhibited the beginning the recessional limbs (Figure2); the second and third peaks followed precipitation events, representing a flushing/remobilization of the tracer. The arrival times of the Cl^- in the well ranges from 14to 21 days. The wells that are farther away from tiles experienced longer arrival times than the wells that are closer (Table 2)

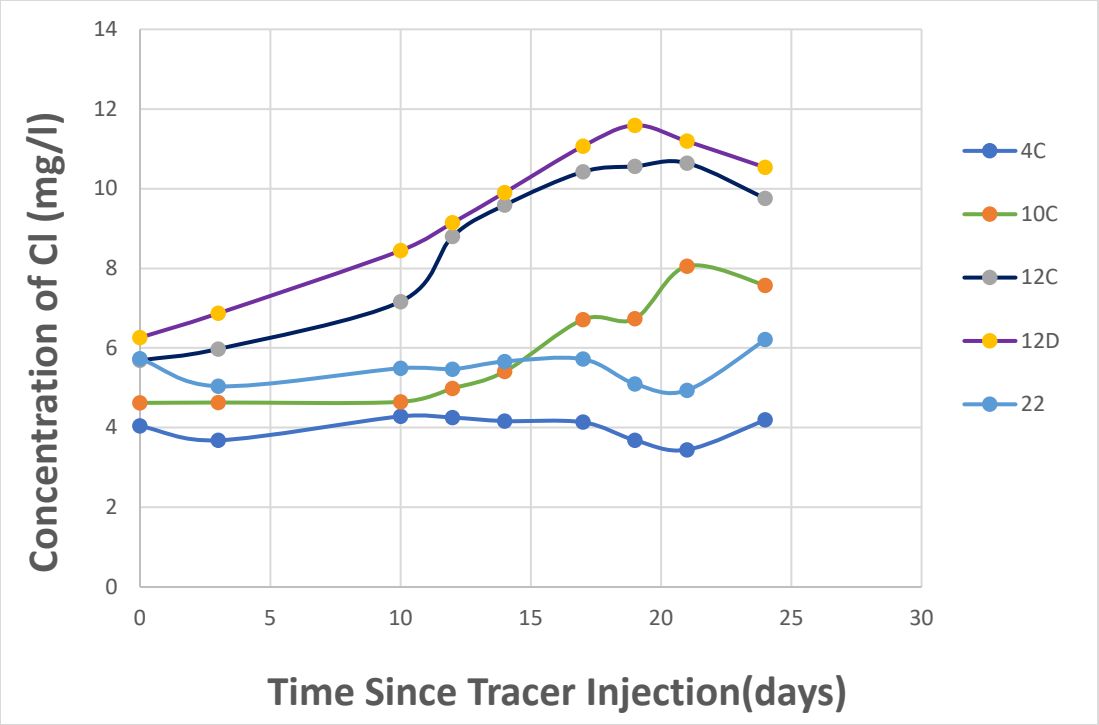

Figure 7: Representative breakthrough curves from the tracer test, the breakthrough curves for wells 4C, 10C, 12C, 12D and 22 are represented. The arrival times are taken from the peak of the curves.

Hydraulic Gradient Data

The hydraulic gradient of the head of groundwater in the site generally increases as one moves towards the stream. The gradient was highest towards the wells closer to the diversion tiles and becomes lower further away from the tiles. The hydraulic gradient was used in the determination of the travel distances. The hydraulic gradient became more steeper as the test progressed in time due to the increase in the influx of tile waters. The figure below shows the hydraulic gradient on

the beginning of the tracer test on 3-13-2021 and the end of the tracer test on 4-13-2021. The other figures of the hydraulic gradients for the rest of the days are in the appendix (appendix C).

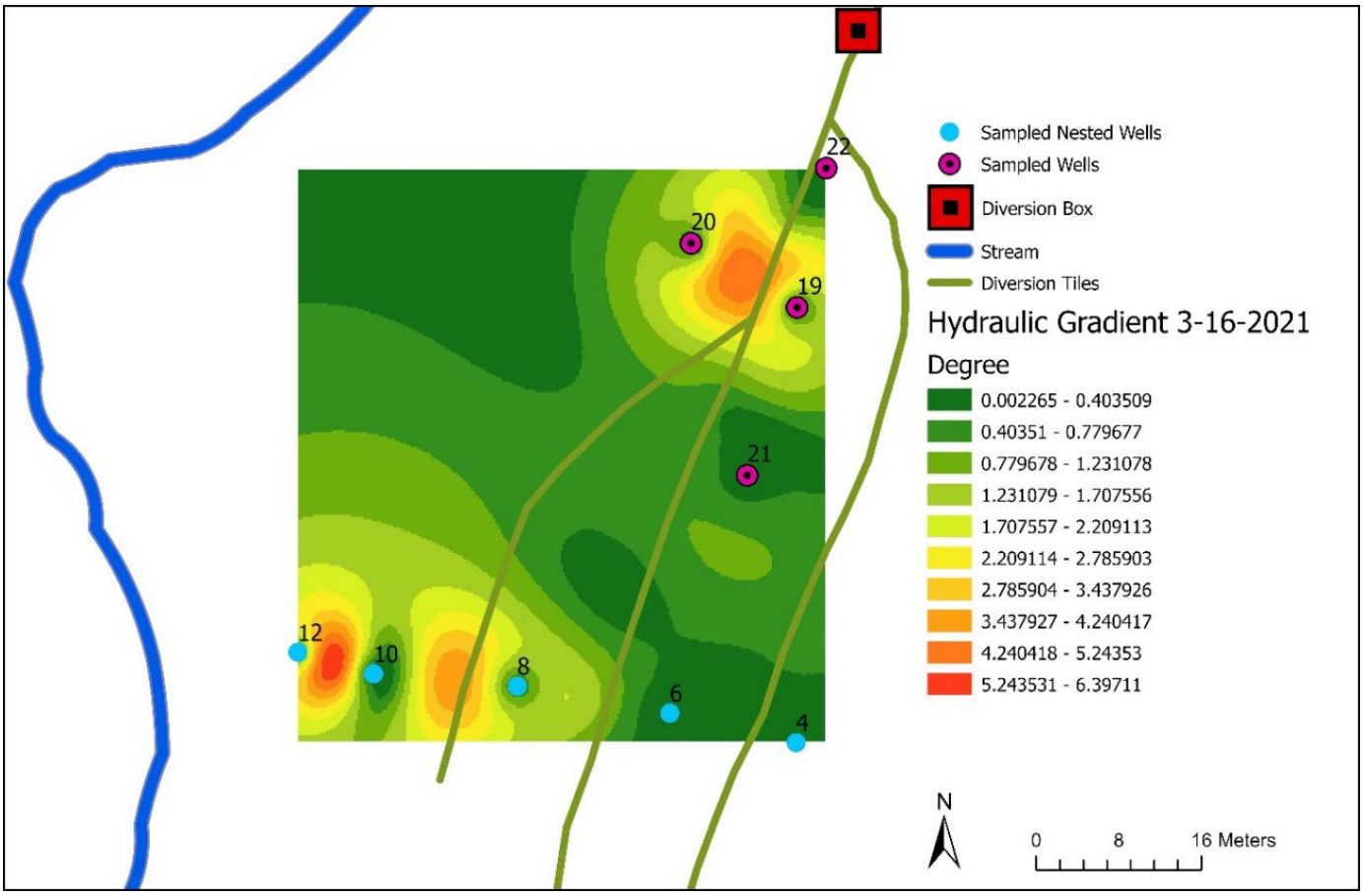

Figure 8: Hydraulic gradient of head of water on the first day of sampling in degrees

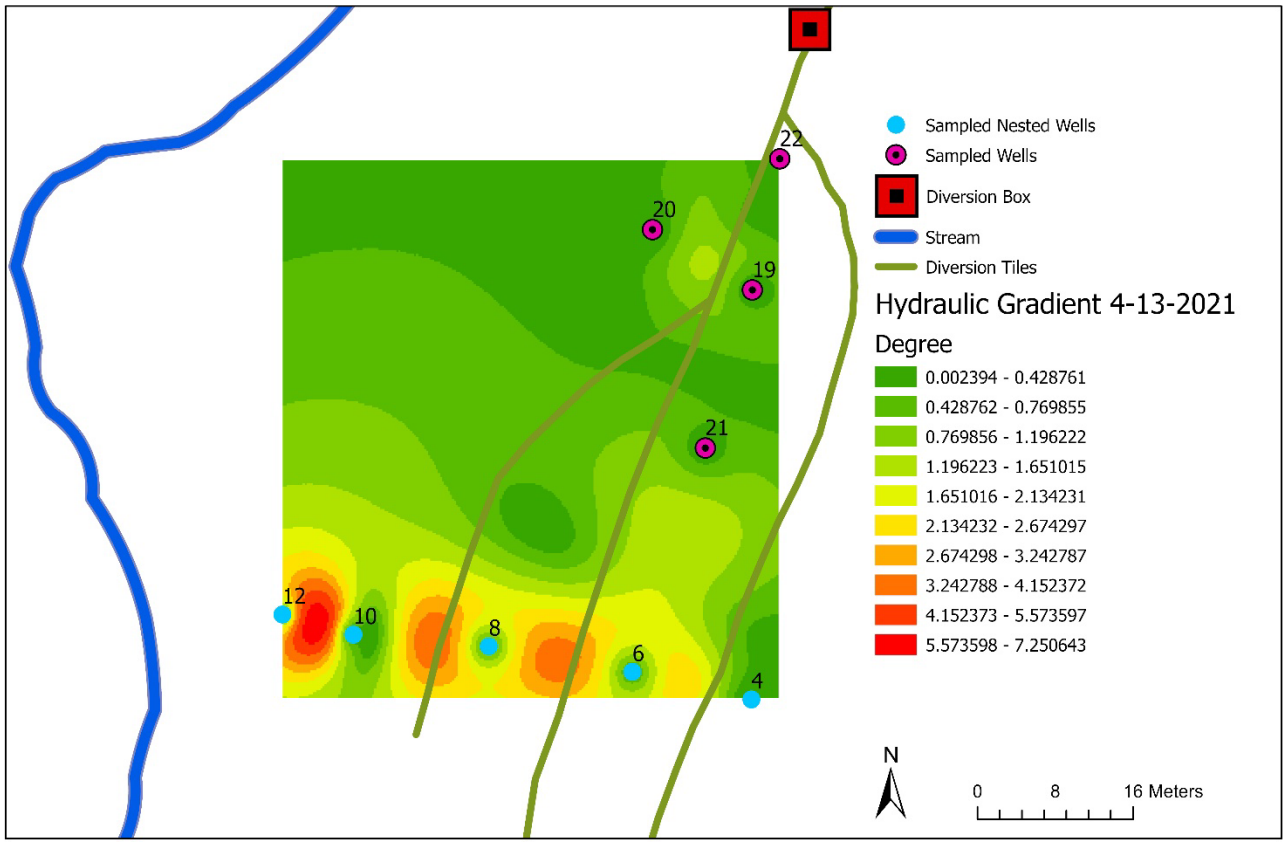

Figure 8: Hydraulic gradient of gradient water on the last day of sampling in degrees

From the hydraulic gradient maps, the travel distances were computed through the line with the steepest slope. This is because the flow velocities will be highest along travel distances with the steepest slope.

Table 3: Travel Time of the tracer from the closest tiles to the wells. ET is Easting Diversion Tile; MT is the Middle diversion Tile and WT is Western diversion tile

Well	Distance from Nearest Tile(m)	Travel Time(days)
8C	`6.53	17
8D	5.49	17
10C	6.86	21
10D	6.76	19
12C	12.83	21
12D	11.77	19
19	7.74	19
20	6.31	17
21	7.54	17
22	2.49	14

The variation of travel time with distance away from the closest diversion tile produced an exponential model (distance-travel time model) with the equation

$y=11.948x^{0.21}$ Eq (8)

where x is the distance away from a diversion tile and y is the travel time as shown in figure 4.

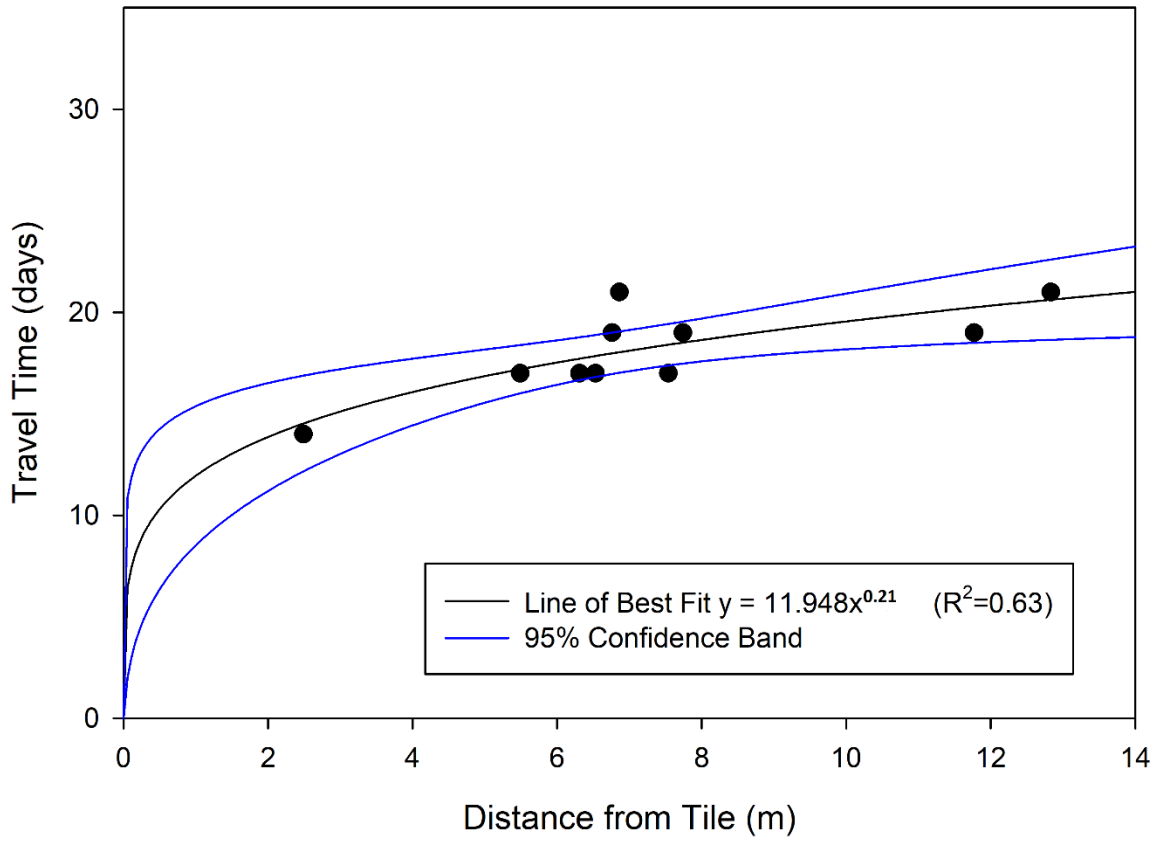

Figure 9: Arrival times of the Cl- to the various wells against the closest distance to those wells. There is an exponential relationship between distance from tile and travel time of tile waters

Calculated K values, using eq (2), ranged from 1.15×10^{-4} m/s to 3.29×10^{-3} m/s with an average of 7.44×10^{-4} m/s. These values algin well with the slug test (Figure 5). The average groundwater velocity was 0.36 m/day±0.19m/day. The conformity between the tracer hydraulic conductivity and field hydraulic conductivity further validates the results obtained from the tracer test.

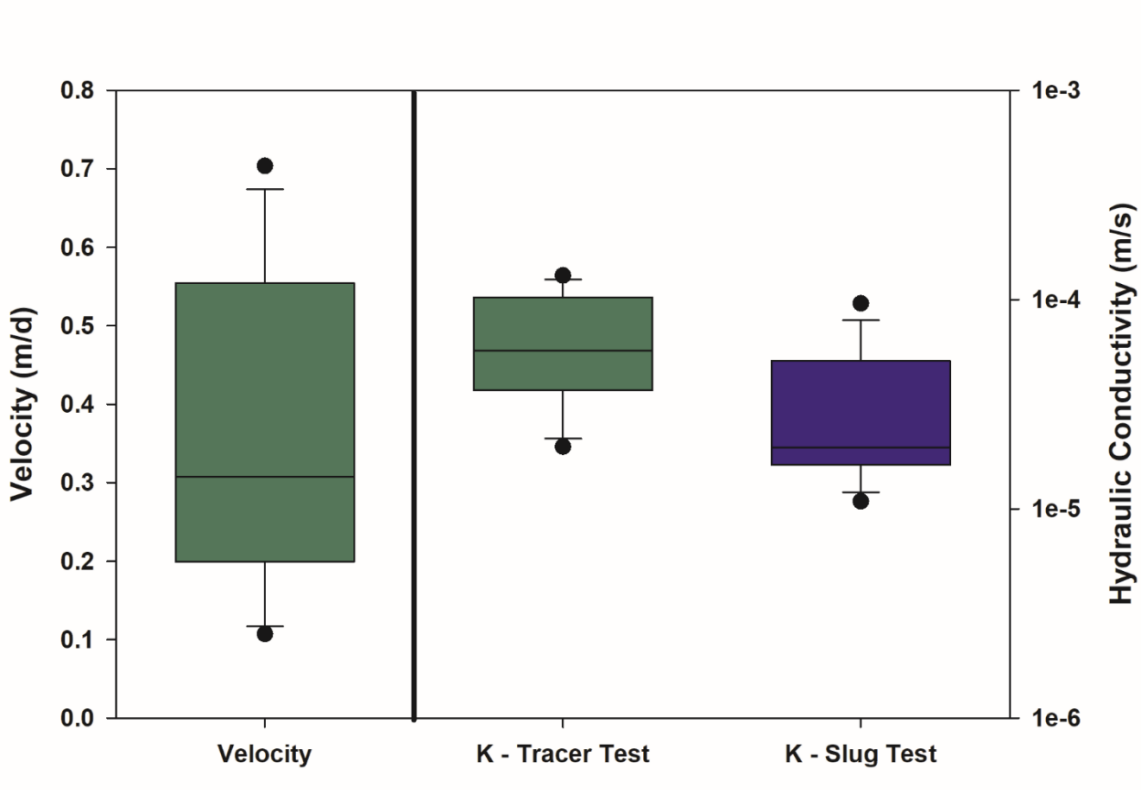

Figure 10: Groundwater velocity and hydraulic conductivity obtained from both tracer and slug test. There is a general conformity between the tracer test results and the tracer test results

Mixing Model

Results from the mixing model are grouped into two-sets. The first set resulted from quantifying the proportion of tile water to groundwater in the well water (Eq. 5) and the second set was generated from finding the amount of reduction in the concentration of the NO_3-N in the well water (Eq 7). The table below shows the summary of the proportion of tile waters that the well waters were composed of during the test/

Table 4: Descriptive statistics of the proportion of tile water found in the sampled wells relative to the groundwater during the test. Values greater than 100% indicates that on those days, the proportion of tile waters fell outside the end members of the mixing model

Well	min	average	max	std
8C	7%	32%	82%	26%
8D	16%	22%	65%	27%
10C	34%	43%	60%	12%
10D	29%	53%	68%	15%
19	9%	36%	76%	31%
20	39%	68%	113%	27%
21	26%	53%	102%	27%
22	6%	28%	91%	29%

It can generally be seen that the wells that are closer to the diversion tiles such as wells 8C and 8D, 19 has higher percentage of tile water in them. However, even though well 22 is closer to a tile, it still had lower percentage of tile water in some days. A basic descriptive statistic performed on the amount of tile water in the wells shows there is high variation in the amount of tile water in well 19 with least amount of variation in the tile water occurring in well 22 as shown in the Table4.

The second part of the mixing model is the data on the amount of reduction of NO_3-N that occurs in the wells during the various times measurements were taken as computed using eq (5).

Table 5: Descriptive statistics of the difference between modeled and measured concentrations of NO_3-N during the various sampling

well	min	max	average	Standard Deviation
8C	41%	81%	68%	14%
8D	4%	58%	29%	22%
10C	3%	26%	16%	10%
10D	-114%	42%	-20%	55%
12C	-6%	-1%	-4%	2%
12D	-30%	10%	-9%	18%
19	5%	82%	42%	31%
20	-40%	42%	3%	29%
21	91%	97%	94%	2%
22	-22%	90%	49%	39%

The measured NO_3-N concentrations in the wells were compared to the modelled concentrations calculated from the mixing model. The modelled NO_3-N was determined using eq.(4) by incorporating the travel time of Cl to the various wells. The travel times were incorporated to make sure that the right Cl^- from the tile and Cl^- from the groundwater system(4C) are used are used in the calculations. This resulted in a limited set of the data because the calculation of NO_3-N could only start after the days the Cl^- arrived in those wells. Most of the wells that were sampled and at most of the days, the measured NO_3-N was less than the modeled, which implies some loss (removal) of NO_3-N has occurred, and are represented by the points which lied below the 1:1 line in fig. (6)

The points that fall above the 1:1 line on fig (6) shows the days were the measured NO_3-N was greater than modeled NO_3-N, which implied there has been addition of NO_3-N(nitrification).

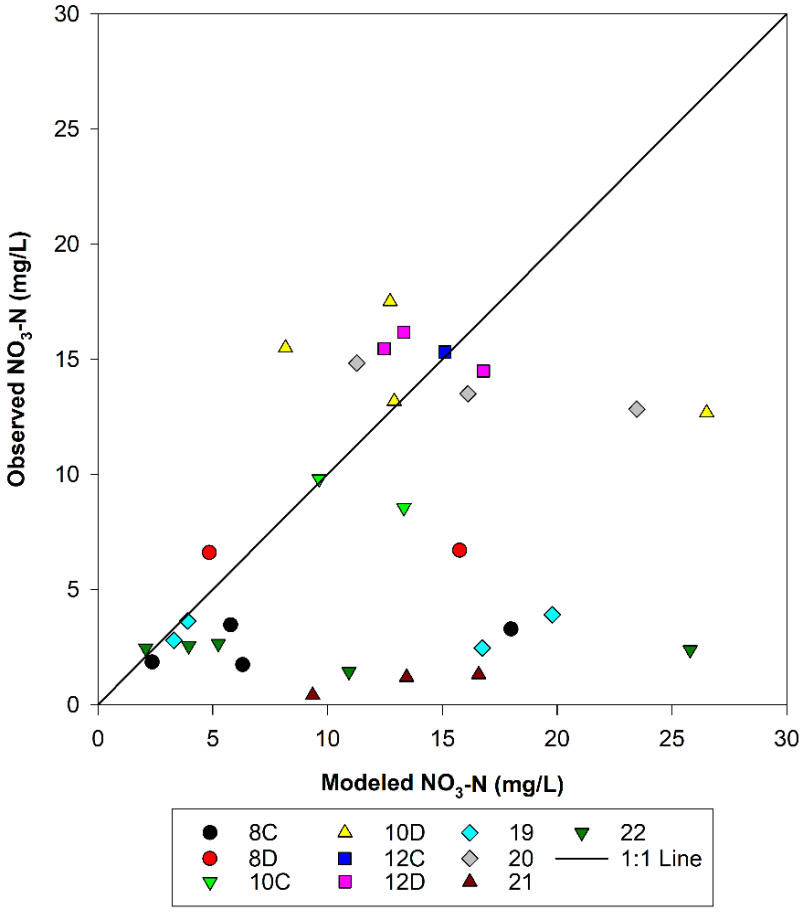

Figure 11: Measured nitrate against modeled nitrate. Points above the 1:1 line indicates addition and points below the 1:1 line represents removal of nitrate. Points on the line represent dilution.

Variation of NO_3-N Concentration with Distance

There was no clear trend in the variation of NO_3-N removal with distance from the tile. Generally, there was more reduction as one moves away from the diversion tiles in wells such as

8C, 8D, and 21. However wells closer to the stream 12C and 12D had nitrate being added contrary to the trend we might expect.

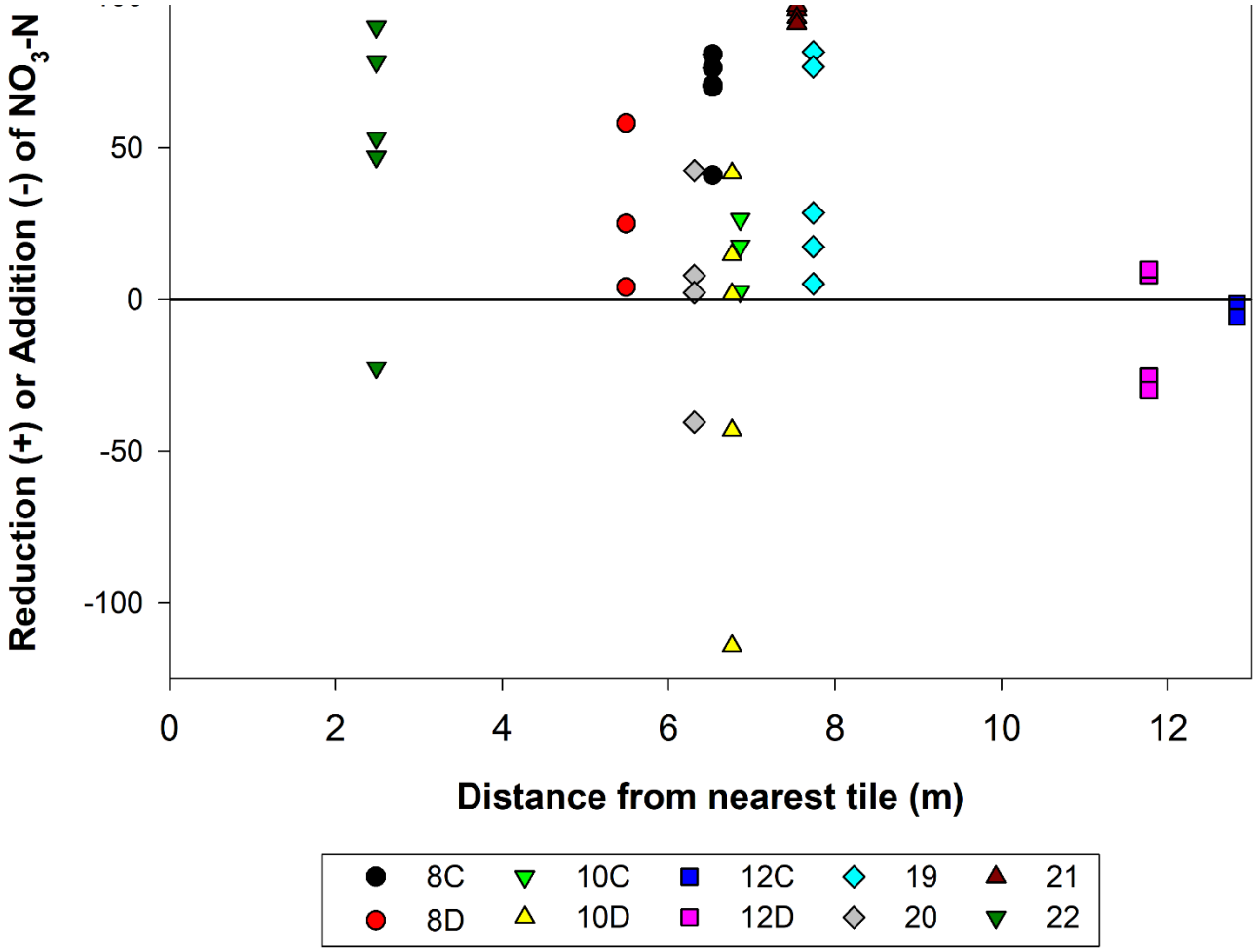

Figure 12: Variation of nitrate with distance away from distribution tiles. The points above the zero line indicates reduction of nitrate and the points below the zero line indicates addition of nitrate.

CHAPTER IV: DISCUSSIONS

Employing the exponential relationship between travel time and distance from diversion tile (distance-travel time model), Eq (8), the travel times of the tile waters from the three diversion tiles to the stream was deduced. The travel time of waters from the western diversion tile (23.45m away from stream) is 23 days. Similarly, the travel time of waters from the middle tile (33.86 m from stream) to the stream is 25 days and that from the eastern tile (43.95 m from stream) is 27 days. 45.3 m represents the maximum width of the SBZ, and therefore, the total travel time of the tracer within the SBZ was calculated to be approximately 27 days using the model in (eq.8). Assuming the transport and behavior of Cl^- and NO_3^--N to be the same, this will mean that the NO_3^--N remains in the system for 27 days. This has very a good implication on the management of because the amount of time the NO_3^--N stays in the SBZ is related to how much of it is removed (Streeter and Schilling, 2021).

Within the SBZ, NO_3^--N removal can occur via various processes including denitrification of NO_3^--N to N_2 or N_2O gas, plant uptake, microbial assimilation, dissimilatory NO_3^--N reduction to ammonium(DNRA)(Lutz et al., 2020). These processes take time to occur, and the time required for tile waters to move through the SBZ is the main reason for the introduction of SBZ as a nutrient reduction strategy. Streeter and Schilling, (2021) quantified the effectiveness of a SBZ to reduce tile NO_3^-N concentrations in eastern Iowa and found out that denitrification would begin to occur in less than a day. The study further found a 10-fold reduction from 15 mg/l NO_3^-N to 1.5mg/l within a span of 7 days, which indicates a significant removal. So therefore

the 27 days that was obtained from the T3 site will be more than enough for much of the NO_3^-N to removed.

The travel time of NO_3^-N depends on the size of the SBZ; Bigger SBZ's will have a longer NO_3^-N travel time and vice versa. With the information on the size of the SBZ and the travel time known, it is very useful because this information can easily be applied in other areas to determine the optimal size of land to be used in the implementation of SBZ in those areas. This will prevent the wastage of land in SBZ implementation.

The results of our distance-travel time model could be applied in the other areas in the implementation of SBZ to predict how long NO_3^-N will travel knowing the distance from a NO_3^-N source. The application of this model will however depend on the similarity in the hydrogeology and geology of that site. This is because SBZs are dependent upon specific soil properties including particle size, hydraulic conductivity, and porosity. It is necessary to assess the specific site characteristics before any implementation in other areas.

NO_3^-N Reduction or Addition

From the mixing model, it can be observed that the wells that were closer to the diversion tiles, such as 19 and 22 to be composed of 100% of tile water, in some days. This makes sense because of their proximity to the diversion tiles, which makes them inundated by tile water in most of the time. The contribution of the tile water to the well water in some of the days were greater than the 100%. Values greater than 100% implies that the Cl^- concentration in those wells on those days were beyond the end member concentrations of the mixing model. This means that the measured Cl^- in those wells were greater than the measured Cl^- in in the tile waters. This is

attributed to the use of lag time during the calculation of the model, which resulted in days that sampling did not take place, the closest day of sampling was used in those cases, and this resulted in the above-mentioned error. This is a limitation of the mixing model usage; a similar limitation is reported by (Anderson et al., 2014), and this was due to the frequency of sampling, which is a similar issue observed in our test.

Variation in NO_3^-N removal and addition data

Generally, wells that are far away from diversion tiles have higher the NO_3^-N removal than wells that are closer to the diversion tiles; however, wells such as 12 C and 12 D even though are the farthest from the wells had NO_3^-N being added. The possible reason for this is the movement of the built-up nitrate within the system. The decay and degradation of plant material during the fall and winter has been documented to generate nitrate in the unsaturated zone (Bosompemaa et.al, 2020). The movement of the built-up nitrate within the system interacts with the water in the unsaturated zone, leading to the addition of nitrate in that area. The tracer test was conducted in the Spring where you have an accumulated dead plant biomass, and the upwelling water could carry this to those wells. Additionally, similar research conducted by Anderson et. al, (2014) showed that there was no strong relation relationship between the amount of NO_3^-N removed and distance away from diversion tiles. They observed some wells closer to diversion tiles, which had higher nitrate removal, and their results compares quite well with the results from our test.

The data from the from the mixing model show times during the tracer test where NO_3^--N was added in a wells and other times when NO_3^--N was being removed. The points in figure 10 which

lie below the zero line indicates NO_3^-N addition. These points could also be because of the variation in the data produced from the mixing model and not just NO_3^-N addition. However, a careful look into the mixing model data reveals that the points below the zero-line occurred at the initial stages of the test. During the initial stages of the test, the tile waters moving through the system carries the built up NO_3^-N from fall and winter seasons. Therefore, it makes sense that the NO_3^-N addition occurred during the initial stages of the tracer test, and it can be confirmed that the observed NO_3^-N addition occurred rather than just a variation in the data.

The possible causes of the NO_3^-N reduction as observed by the mixing model are denitrification and plant uptake (Bosompemaa et al., 2019; Miller et al., 2019). Denitrification leads to the permanent removal of NO_3^-N, while the plant uptake is a temporal removal of NO_3^-N. Groh et al., 2018 assessed in situ denitrification within SBZs via acetylene inhibition method and found out that denitrification accounted for between 4 to 77% of the total nitrate removed within the SBZ. The occurrence of denitrification requires anaerobic conditions and labile organic carbon. When the agricultural runoff enters the SBZ, the runoff displaces oxygen in the soil, which makes the soil saturated water and hence, creating anaerobic conditions. The average measured dissolved oxygen during the period of the tracer test is 4 mg/l as shown in table(1). Streeter and Schilling (2021) observed that denitrification is mostly dominant when the dissolved oxygen rate within SBZ ranges from 2 mg/l to 4.5 mg/l. This clearly implies the study site had the required anaerobic conditions required for denitrification to take place. Jaynes et. al 2019, reports that for denitrification to take place in a SBZ, at least 1.2% of the soil by mass must be organic carbon. The geology of the study is made up of a 2m with very rich organic carbon. Bosompemaa et al. (2019) reported an average organic matter content at the study site to 6.0% at a depth of 60 cm.

This clearly indicates there is enough organic carbon for denitrification to occur on our study site. Plant uptake is also a contributing factor to the observed denitrification on the site. The study site is dominated by switch grass. Bransby et al. (1998) reported that switchgrass can recover 66% of applied nitrogen, though this is very minimal because the plants were just starting to grow during the period of the tracer test.

The possible cause of the nitrate addition can be attributed to the roots of the plants that decomposes as well as the dead plants found within the soil. These decomposed plants return the assimilated nitrate back into the soil and this could result in nitrate addition in some days. Miller et al. (2019) observed some nitrification on some days on the study site in research that was conducted on the site to assess the seasonal and diurnal variation of NO_3^-N on the study site. Also, the time of the year that the research was conducted, Spring could be a contributing factor to the observed nitrification as there is an accumulated nitrate stored in the Buffer zone from the previous growing season and since the test started just when the tiles started flowing, the tile water could carry the accumulated NO_3^-N along.

CHAPTER V: CONCLUSIONS

The results from the tracer test suggests that time is a very important component in the nitrate removal from Saturated buffer Zone. The distance-travel time model produced ($y=11.948x^{0.21}$, $R2=0.63$) could be used to give an idea of how the travel time of NO_3^-N might be in a similar

geologic material. Total travel time of NO_3^-N from the SBZ to the stream is 27 days which corresponded to an overall average of 43% reduction in nitrate removed from the SBZ, this is a significant reduction compared to previous studies in other areas as compared to the long-term goal set out by the Illinois Nutrient reduction Strategy, which is to reduce NO_3^-N load by 45 % by the year 2025. Denitrification is the most possible mechanism responsible for the NO_3^-N removal within the SBZ based on the soil nature of the soil and the groundwater chemistry conditions. This study could be employed in other areas, but additional studies need to be conducted to ascertain the site-specific hydrologic activities. This study further reinforces the effectiveness of SBZ in nitrate removal

Future Work

In the future, another tracer test could be conducted on the site which in cooperates the measure of fluxes of tile water entering the SBZ. Pressure transducers as well as the V-notch within the diversion box could be used to measure the fluxes of water moving into the SBZ. This will make it possible to calculate the load of nitrate coming into the SBZ to quantify the amount of NO_3^-N removed or added. This might be a good estimate of NO_3^-N addition or removal.
Additionally, the tracer test could be conducted in other times of the year to investigate the effect of seasons on the results obtained.

REFERENCES

Anderson, T. R., Groffman, P. M., Kaushal, S. S., and Walter, M. T., 2014, Shallow Groundwater Denitrification in Riparian Zones of a Headwater Agricultural Landscape: Journal of Environmental Quality, v. 43, no. 2, p. 732-744, doi:10.2134/jeq2013.07.0303.

Bosompemaa, P., Peterson, E., Perry, B., and Seyoum, W. M., 2019, Nitrate transport in the unsaturated zone: Geological Society of America Abstracts with Programs, v. 51, no. 5, doi:10.1130/abs/2019AM-339771.

Bransby, D. I., McLaughlin, S. B., and Parrish, D. J., 1998, A review of carbon and nitrogen balances in switchgrass grown for energy: Biomass & Bioenergy, v. 14, no. 4, p. 379-384, doi:10.1016/s0961-9534(97)10074-5.

Carstensen, M. V., Hashemi, F., Hoffmann, C. C., Zak, D., Audet, J., and Kronvang, B., 2020, Efficiency of mitigation measures targeting nutrient losses from agricultural drainage systems: A review: Ambio, v. 49, no. 11, p. 1820-1837, doi:10.1007/s13280-020-01345-5.

Castaldelli, G., Colombani, N., Soana, E., Vincenzi, F., Fano, E. A., and Mastrocicco, M., 2019, Reactive nitrogen losses via denitrification assessed in saturated agricultural soils: Geoderma, v. 337, p. 91-98, doi:10.1016/j.geoderma.2018.09.018.

Chandrasoma, J. M., Christianson, R. D., and Christianson, L. E., 2019, Saturated Buffers: What Is Their Potential Impact across the US Midwest?: Agricultural & Environmental Letters, v. 4, no. 1, doi:10.2134/ael2018.11.0059.

David, M. B., Drinkwater, L. E., and McLsaac, G. F., 2010, Sources of Nitrate Yields in the Mississippi River Basin: Journal of Environmental Quality, v. 39, no. 5, p. 1657-1667, doi:10.2134/jeq2010.0115.

David, M. B., and Gentry, L. E., 2000, Anthropogenic inputs of nitrogen and phosphorus and riverine export for Illinois, USA: Journal of Environmental Quality, v. 29, no. 2, p. 494-508, doi:10.2134/jeq2000.00472425002900020018x.

Galloway, J. N., Aber, J. D., Erisman, J. W., Seitzinger, S. P., Howarth, R. W., Cowling, E. B., and Cosby, B. J., 2003, The nitrogen cascade: Bioscience, v. 53, no. 4, p. 341-356, doi:10.1641/0006-3568(2003)053[0341:tnc]2.0.co;2.

Gregory, S. V., Swanson, F. J., McKee, W. A., and Cummins, K. W., 1991, AN ECOSYSTEM PERSPECTIVE OF RIPARIAN ZONES: Bioscience, v. 41, no. 8, p. 540-551, doi:10.2307/1311607.

Lutz, S. R., Trauth, N., Musolff, A., Van Breukelen, B. M., Knoller, K., and Fleckenstein, J. H., 2020, How Important is Denitrification in Riparian Zones? Combining End-Member Mixing and Isotope Modeling to Quantify Nitrate Removal from Riparian Groundwater: Water Resources Research, v. 56, no. 1, doi:10.1029/2019wr025528.

Miller, J., Peterson, E. W., and Budikova, D., 2019, Diurnal and seasonal variation in nitrate-nitrogen concentrations of groundwater in a saturated buffer zone: Hydrogeology Journal, v. 27, no. 4, p. 1373-1387, doi:10.1007/s10040-018-1907-y.

Streeter, M. T., and Schilling, K. E., 2021, Quantifying the effectiveness of a saturated buffer to reduce tile NO3-N concentrations in eastern Iowa: Environmental Monitoring and Assessment, v. 193, no. 8, doi:10.1007/s10661-021-09297-3.

Xin, J., Liu, Y., Chen, F., Duan, Y. J., Wei, G. L., Zheng, X. L., and Li, M., 2019, The missing nitrogen pieces: A critical review on the distribution, transformation, and budget of nitrogen in the vadose zone-groundwater system: Water Research, v. 165, doi:10.1016/j.watres.2019.114977.

Zhang, Z. W., Han, Y. X., Xu, C. Y., Ma, W. C., Han, H. J., Zheng, M. Q., Zhu, H., and Ma, W. W., 2018, Microbial nitrate removal in biologically enhanced treated coal gasification wastewater of low COD to nitrate ratio by coupling biological denitrification with iron and carbon micro-electrolysis: Bioresource Technology, v. 262, p. 65-73, doi:10.1016/j.biortech.2018.04.059.

APPENDIX A: CHLORIDE RESULTS

Time (Days)	IC Time	Date\Well	4C	4D	6C	8C	10C	12C	12D	19	20	21	Div. Box
	1_28_2021	1/28/2021	0.39	0.35	0.53	0.51	0.45	0.59	0.00	3.32	4.50	0.80	6.80
	3_04_2021	3/4/2021	0.32	0.34	0.45	0.56	0.44	3.77	4.55	1.65	7.17	1.26	11.44
3	3_16_2021	3/16/2021	0.39	0.42	0.49	0.62	1.19	4.61	4.04	2.30	4.56	0.68	8.32
10	3_23_2021	3/23/2021	0.35	0.37	0.45	0.50	1.69	4.69	5.63	2.72	13.09	0.64	17.70
12	3_25_2021	3/25/2021	0.39	0.41	0.45	0.49	1.74	6.25	7.43	2.82	14.29	0.57	21.94
14	3_27_2021	3/27/2021	0.39	0.41	0.49	0.53	2.38	8.48	9.24	2.86	15.90	0.53	21.79
17	3_30_2021	3/30/2021	0.45	0.40	0.48	0.61	4.34	11.52	12.73	3.04	18.03	0.48	23.85
19	4_1_2021	4/1/2021	0.30	0.39	0.46	0.38	4.44	11.96	15.18	2.93	16.43	0.65	21.13
21	4_3_2021	4/3/2021	0.25	0.31	0.31	0.56	6.93	15.15	16.69	2.73	15.82	0.41	20.56
24	4_6_2021	4/6/2021	0.33	0.33	0.39	1.85	5.75	13.34	16.17	2.79	14.84	0.41	18.57
26	4_8_2021	4/8/2021	0.38	0.39	0.37	1.73	7.93	15.33	15.46	3.63	13.50	1.19	19.05
29	4_11_2021	4/11/2021	0.82	0.92	1.26	3.46	9.80	15.32	14.49	3.90	12.83	1.31	18.09
31	4_13_2021	4/13/2021	0.33	0.35	0.40	3.28	8.55	12.47	11.62	2.46	10.72	0.59	18.13
33	4_15_2021	4/15/2021	1.13	0.34	1.23	5.72	8.44	14.49	13.91	3.94	14.07	1.24	22.90
39	4_21_2021	4/21/2021	0.31	0.37	0.40	5.78	5.67	13.57	12.30	2.56	10.33	0.44	18.00
43	4_25_2021	4/25/2021	0.25	0.32	0.32	5.81	8.05	12.33	9.65	2.23	7.17	0.37	17.42
45	4_27_2021	4/27/2021	0.45	0.50	0.48	4.37	7.18	10.70	8.58	2.21	4.67	0.46	15.25
48	4_30_2021	4/30/2021	0.21	0.27	0.29	2.65	5.02	8.68	6.53	1.43	3.87	0.37	14.21
53	5_5_2021	5/5/2021	0.34	0.36	0.41	0.73	6.92	5.66	3.98	1.55	2.45	0.59	15.74
61	5_13_2021	5/13/2021	n.a.	0.26	0.39	0.69	6.57	8.39	10.31	1.78	16.55	0.33	33.54
75	5_27_2021	5/27/2021	0.32	0.32	1.25	6.84	3.46	21.75	21.14	1.10	16.55	0.59	28.29
87	6_8_2021	6/8/2021	n.a.	n.a.	n.a.	18.15	5.63	20.50	18.28	1.08	11.21	0.00	30.028

APPENDIX B: MIXING MODEL DATA

Table B1: Quantity of tile water mixing with groundwater in the wells

	8C	8D	10C	10D	12C	12D	19	20	21	22
Days										
17										13.00%
19										0.07
21	7.05%			44.14%		46.29%	10.45%	38.98%	32.10%	6.07%
24	21.64%			28.58%		44.28%	12.99%	57.60%	47.85%	17.87%
26	25.02%	16.20%	33.76%	95.62%	53.71%	59.84%	70.81%	84.22%	59.35%	90.83%
29	82.24%	65.40%	60.42%	58.45%	n.a	n.a	76.33%	n.a	n.a	49.27%
31	22.03%	36.26%	35.64%	64.06%	48.53%	53.14%	9.15%	44.97%	25.98%	9.59%

Table B2: Amount of nitrate removed from the various wells in the various sampling days

%NO3 Removed										
Days	8C	8D	10C	10D	12C	12D	19	20	21	22
17										
19										37%
21	76%			-43%		-25%	17%	-40%	96%	-22%
24	71%			-114%		-30%	29%	8%	97%	53%
26	70%	4%	18%	42%	-1%	8%	82%	42%	93%	90%
29	81%	58%	26%	2%	n.a	n.a	77%	n.a		78%
31	41%	25%	3%	15%	-6%	10%	5%	2%	91%	47%

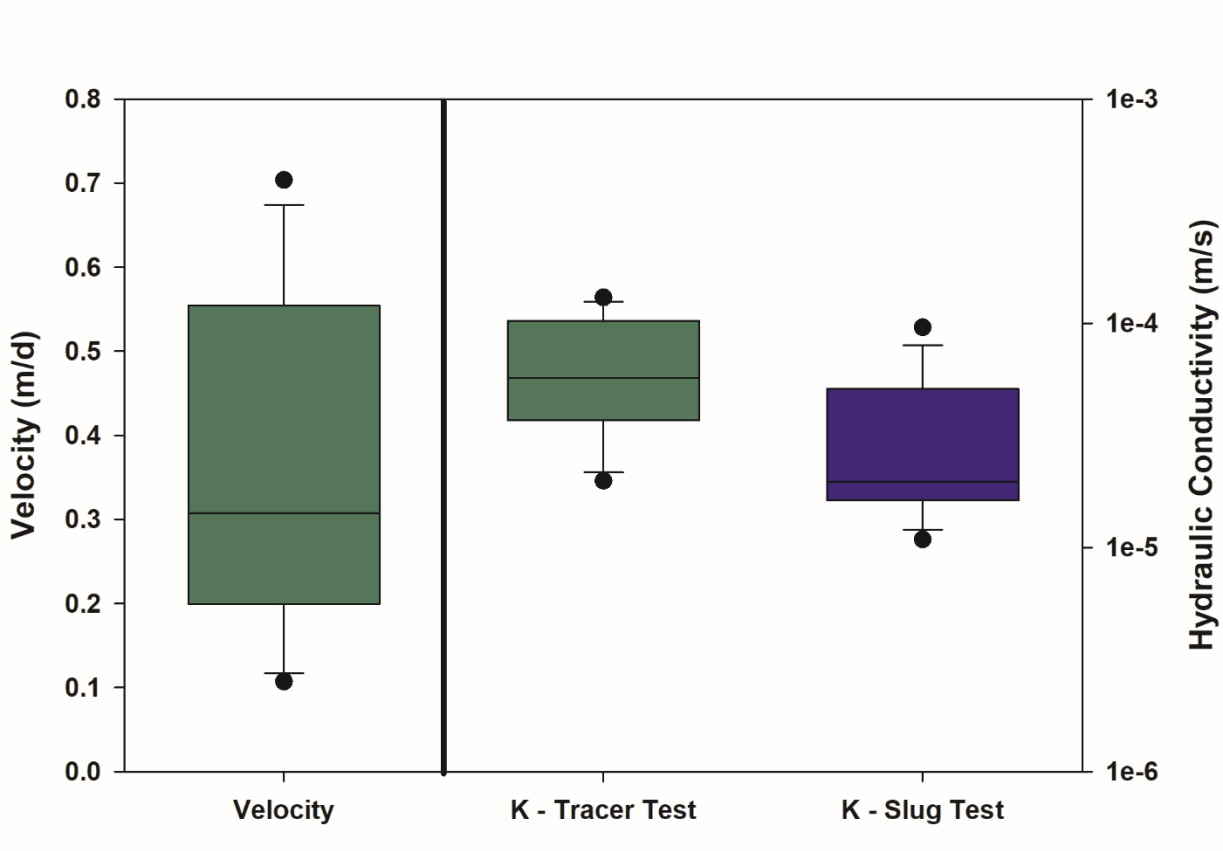

Figure B1-Comparison of tracer test results with field test results

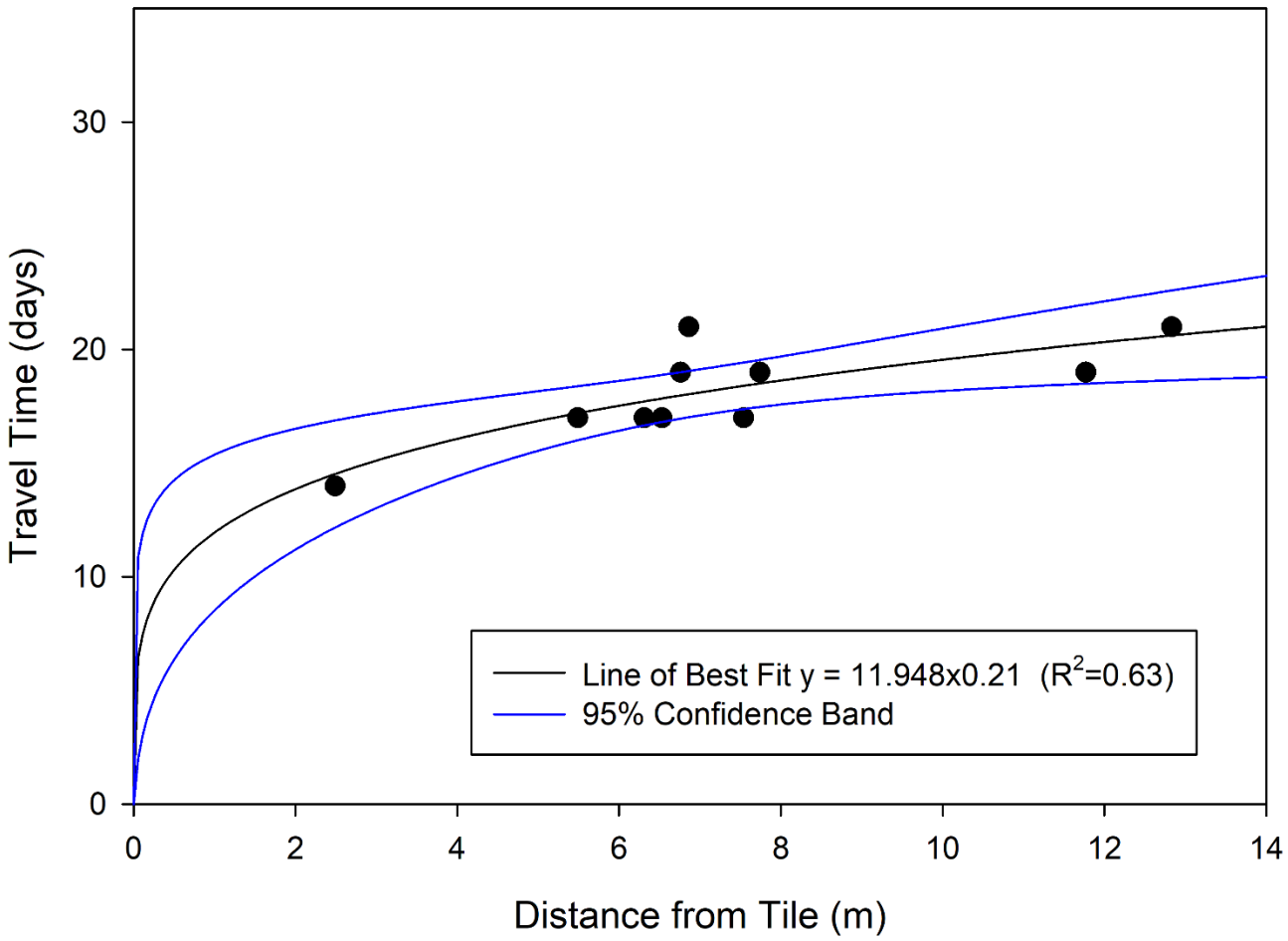

Figure-B2 Relationship between distance and travel time

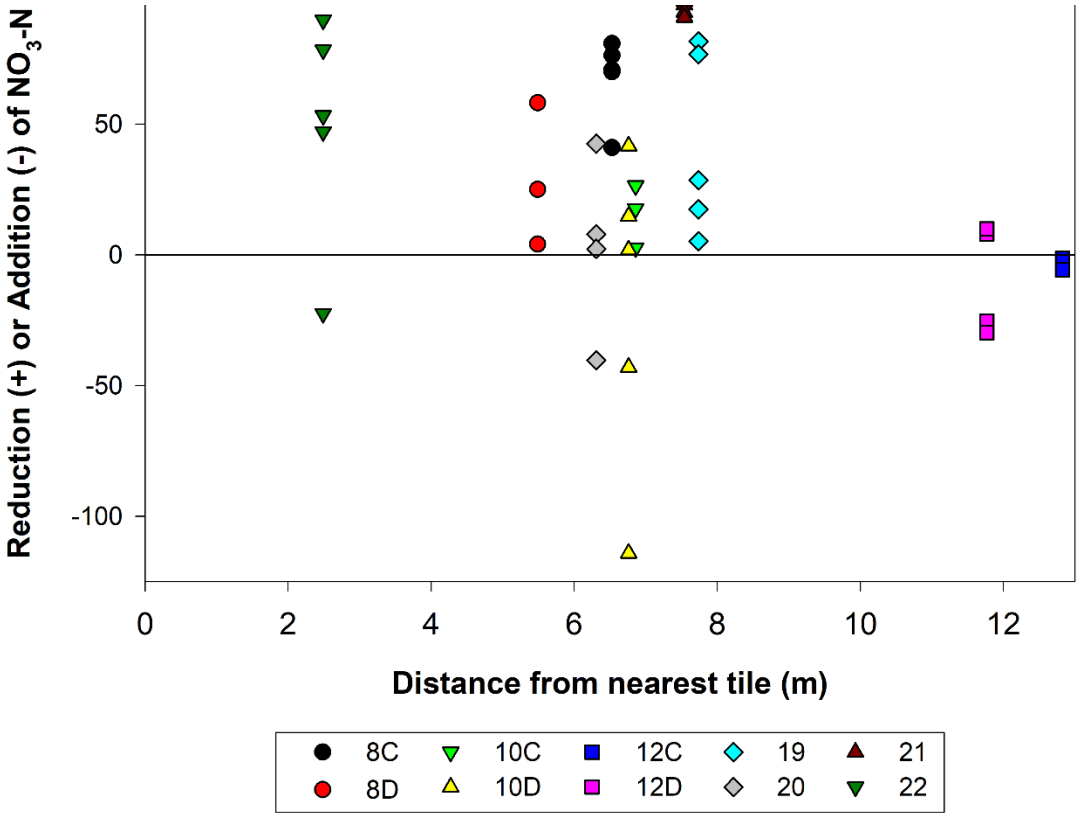

Figure B2: Relationship between nitrate removed and the amount of reduction and distance travelled

APPENDIX C: HYDRAULIC GRADIENT DATA

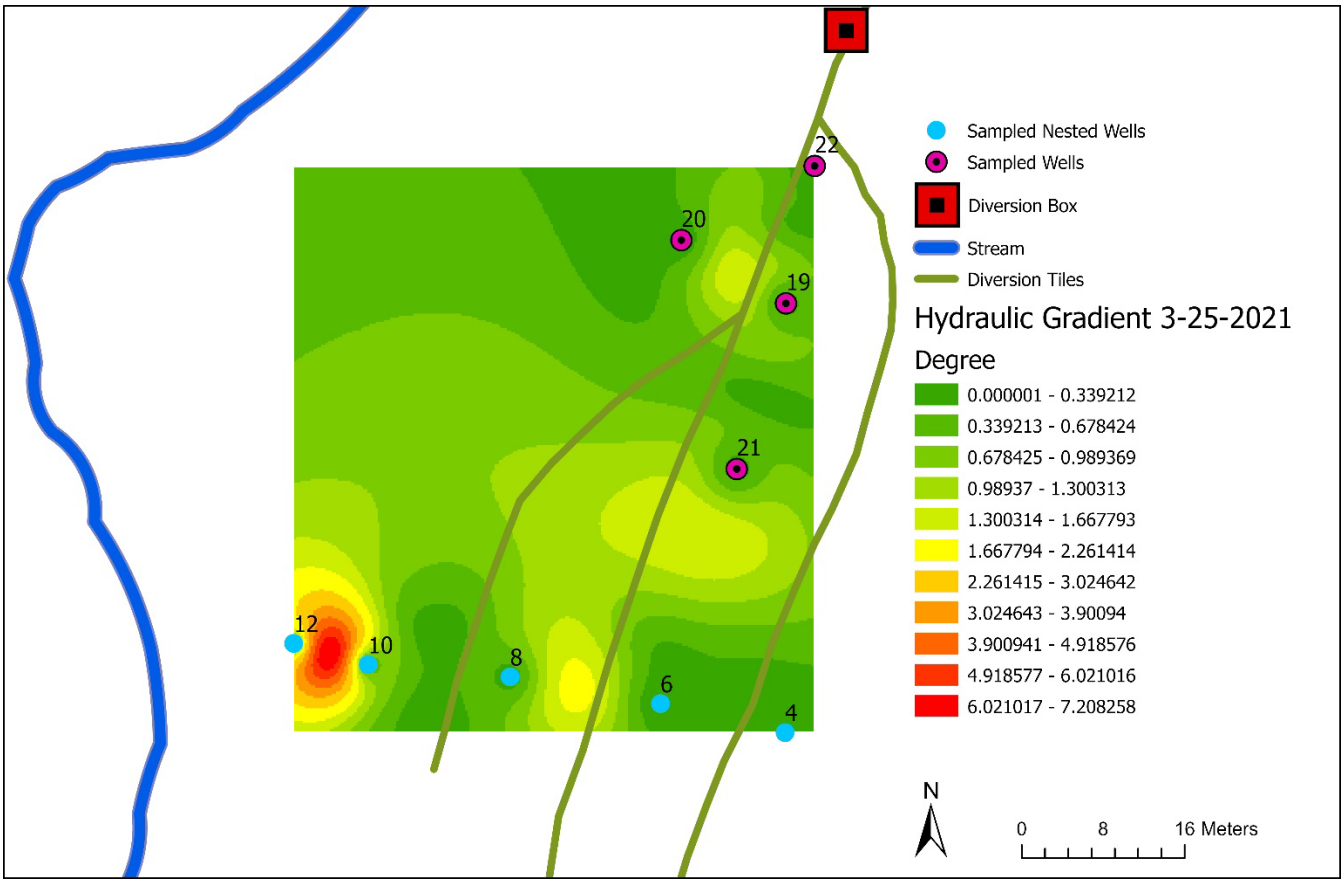

Figure C-1: Hydraulic gradient on 3-25-2021

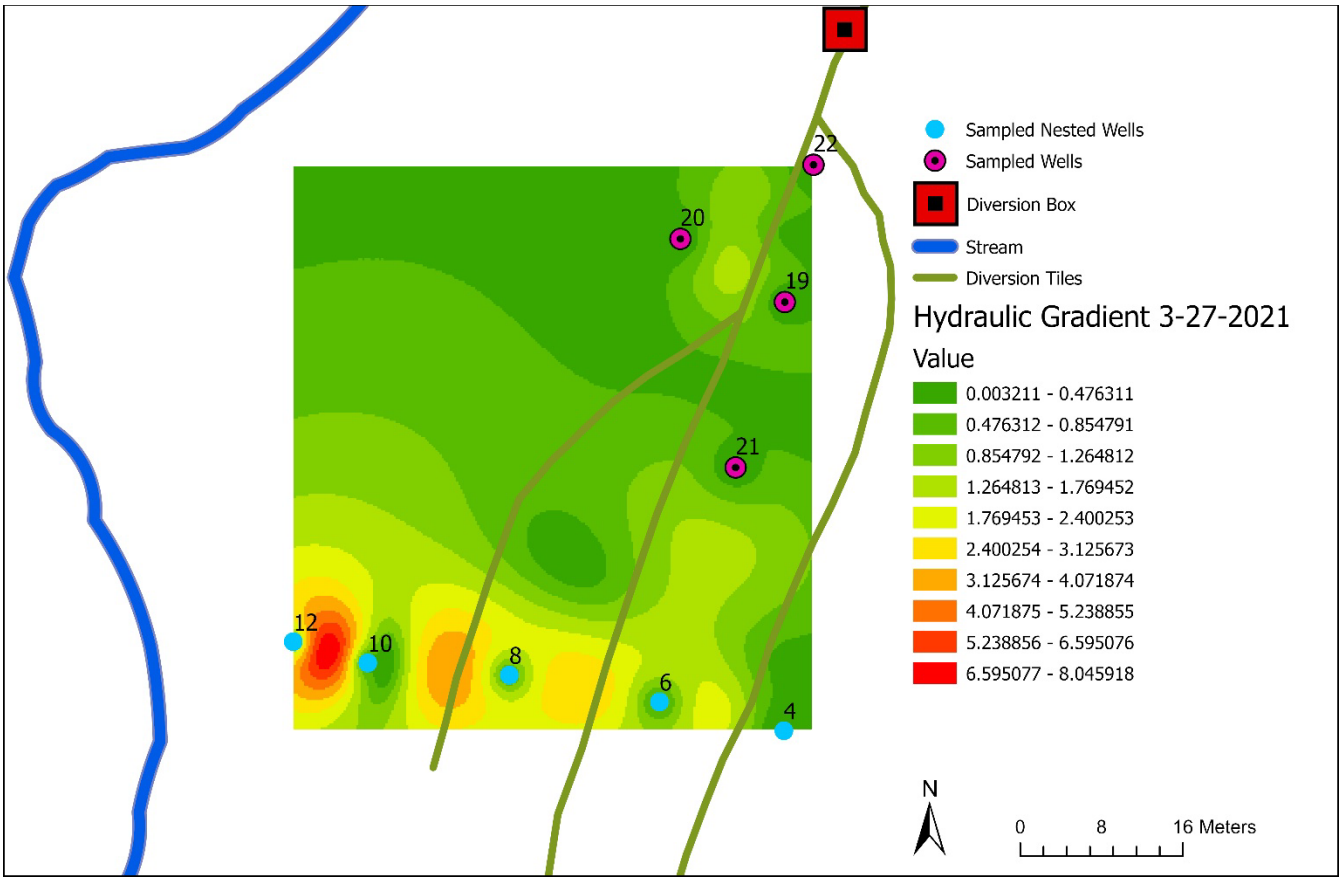

Figure C-2: Hydraulic gradient on 3-27-2021

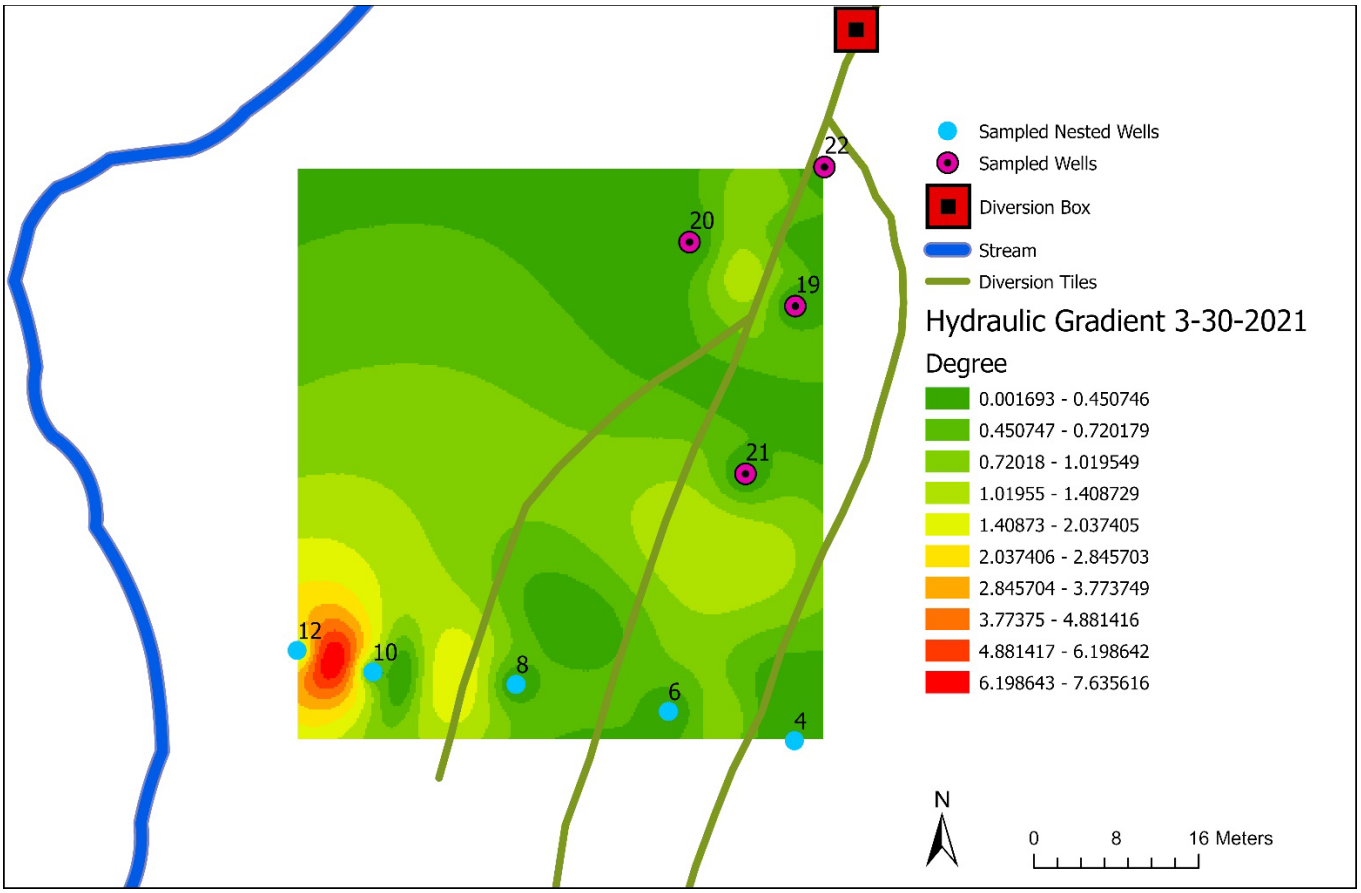

Figure C-3: Hydraulic gradient on 3-30-2021

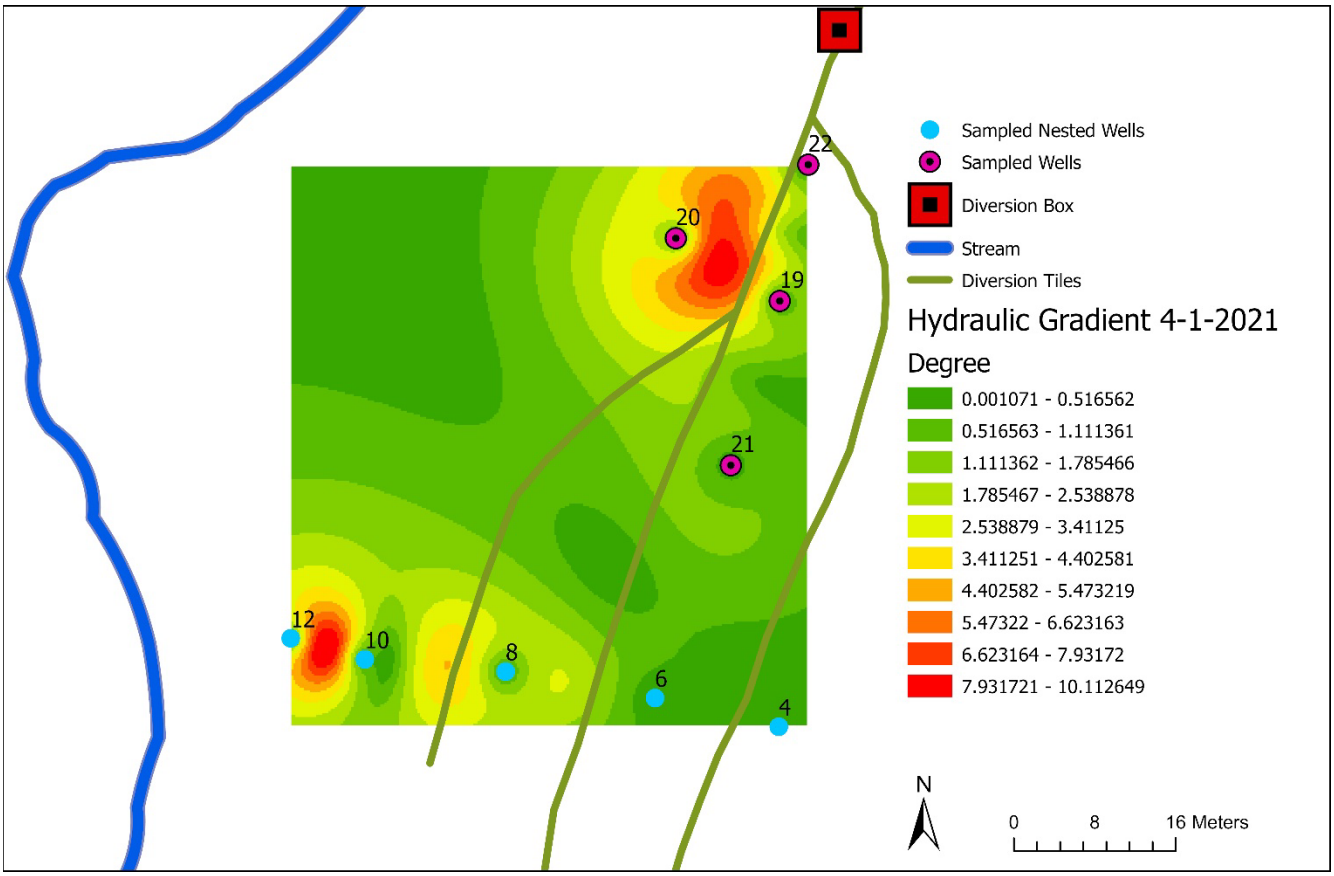

Figure C-4: Hydraulic gradient on 4-1-2021

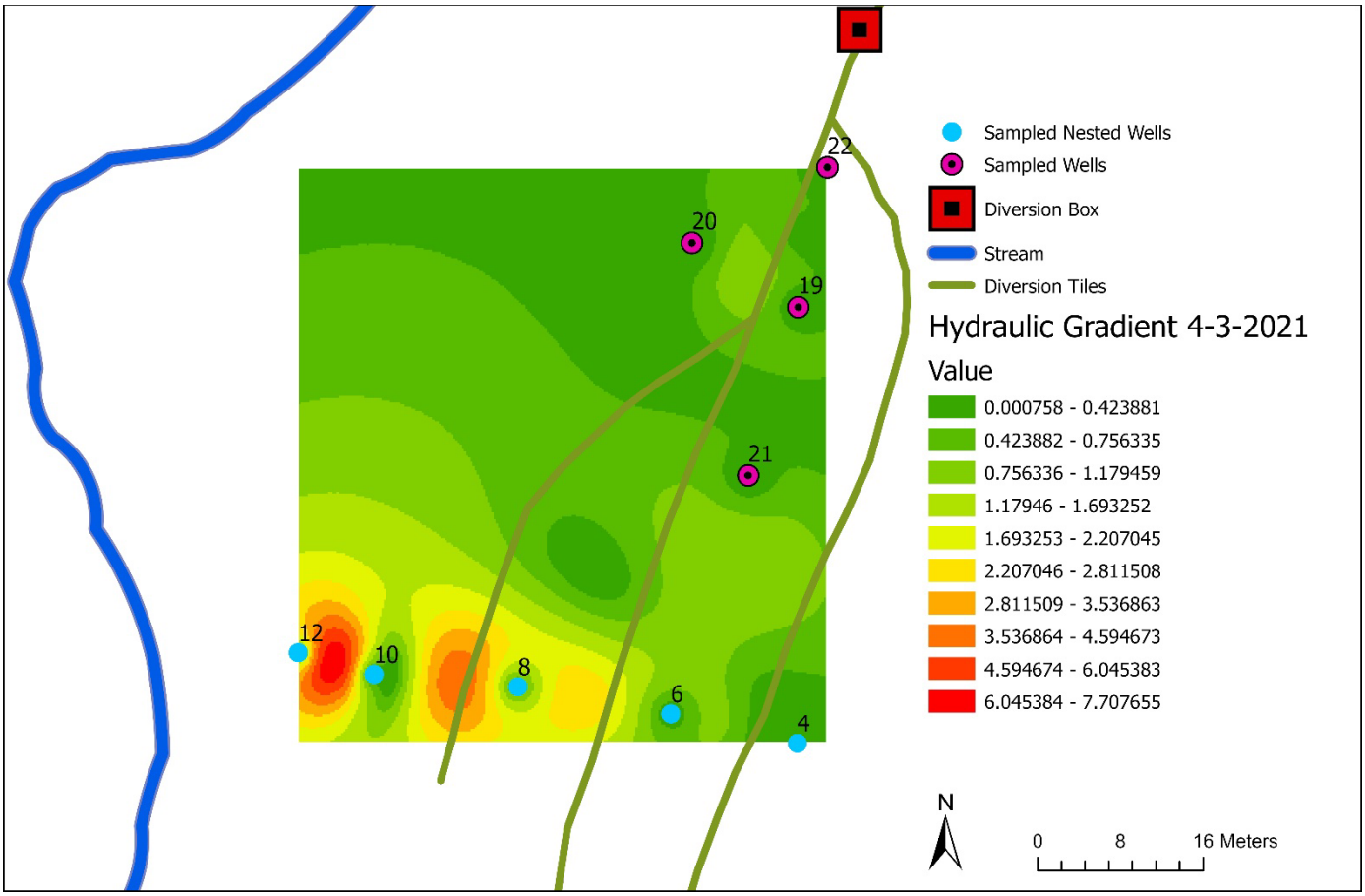

Figure C-5: Hydraulic gradient on 4-3-2021

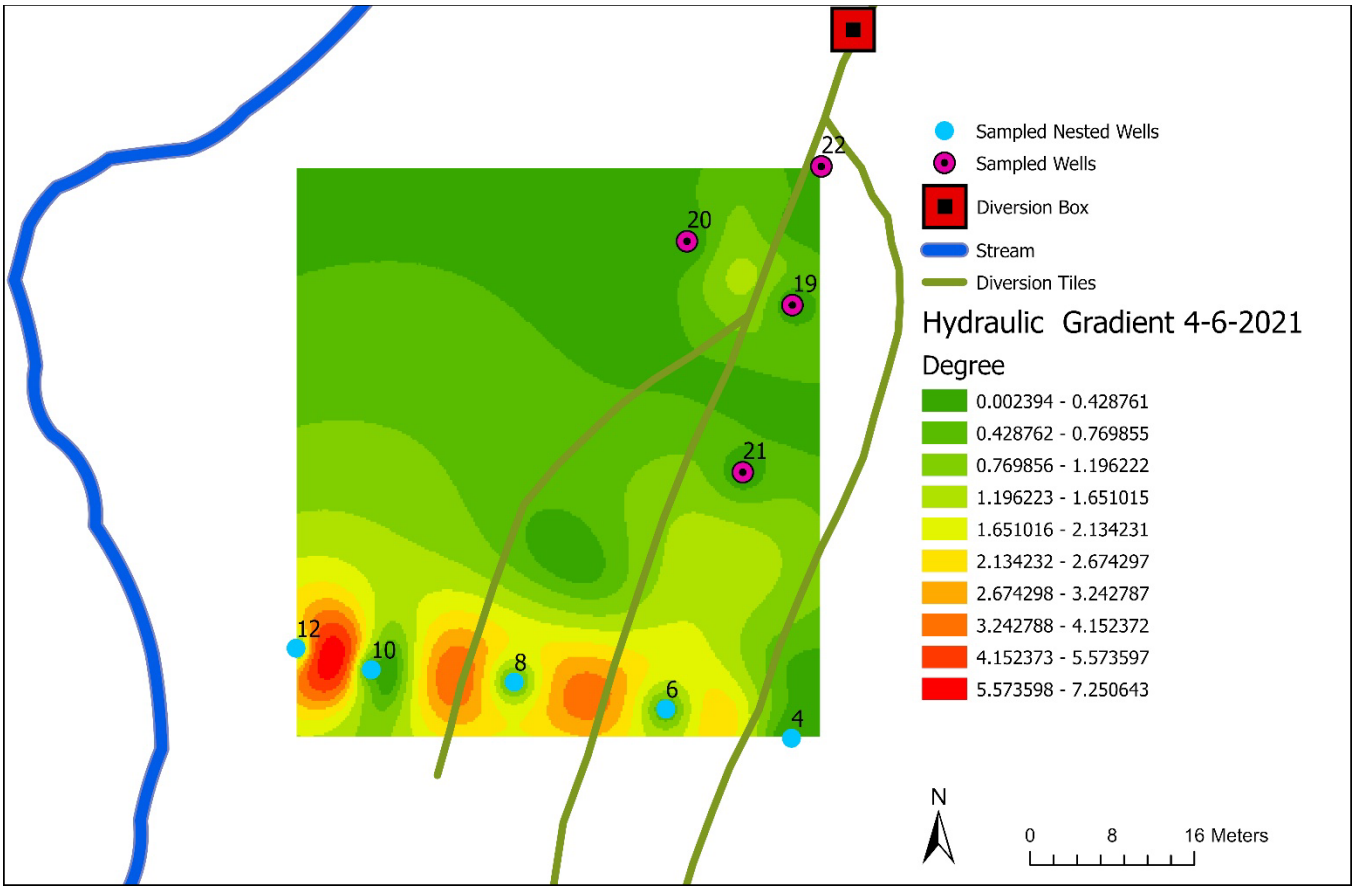

Figure C-6: Hydraulic gradient on 4-6-2021

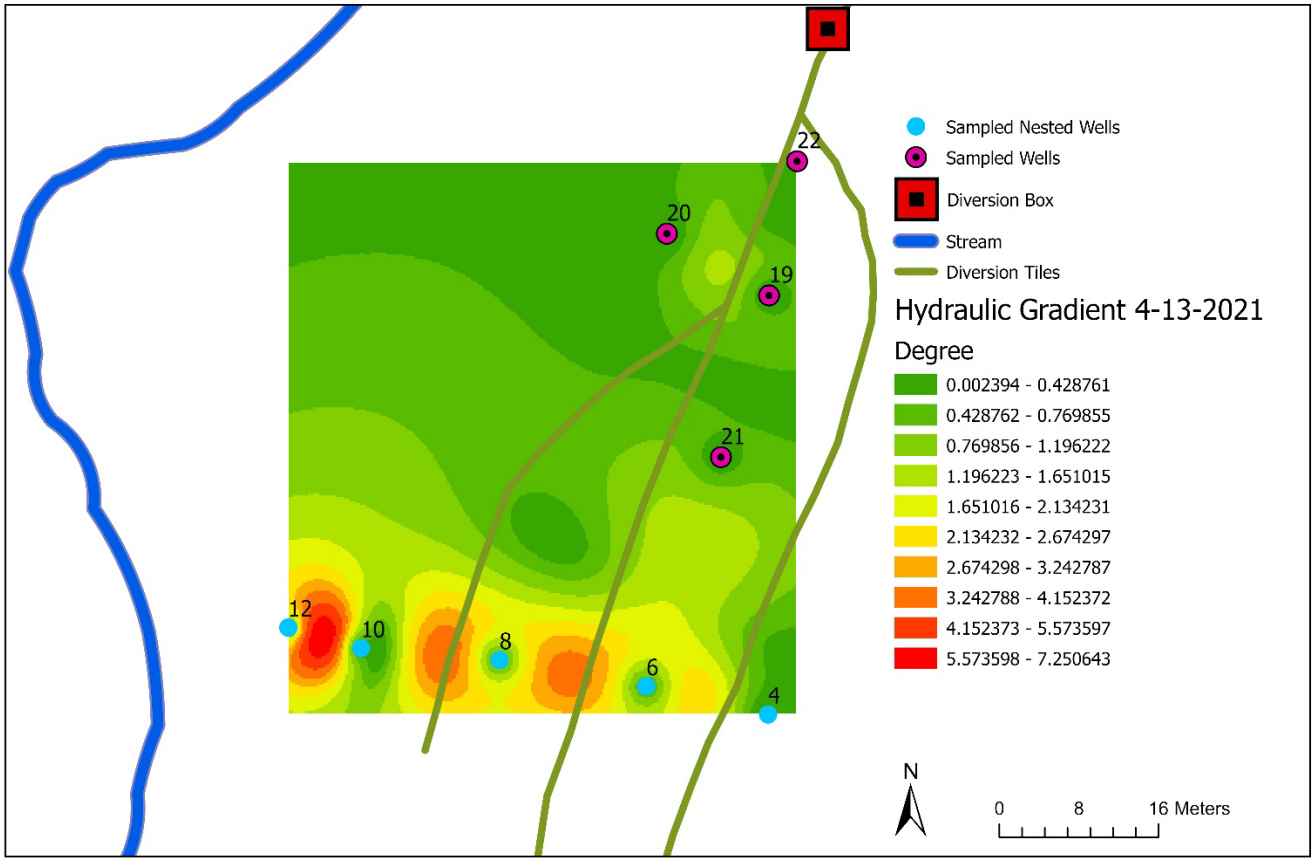

Figure C-7: Hydraulic gradient on 4-6-2021